

Status of strangeness-flavor signature of Quark-Gluon Plasma

Cracov School of Theoretical Physics, Zakopane, June 1/2, 2006

I survey experimental results addressing strangeness observable of quark-gluon plasma, compare briefly with earlier predictions and present its detailed interpretation and analysis. I make an effort to predict the strangeness signature of QGP formation and dynamics at LHC.

Johann Rafelski
University of Arizona
TUCSON, Arizona

Supported by a grant from the U.S. Department of Energy, DE-FG02-04ER41318

- [I] **Introductory remarks: recreating the early Universe in the laboratory**
- [II] **Observing QGP: strangeness and the last 3-5fm/c**
 - Strangeness signatures and results**
 - Strangeness in QGP breakup**
 - Statistical Hadronization**
 - Strangeness as function of centrality and CM energy**
 - Survey of soft hadron production results and analysis insights**
- [III] **Kinetic theory of strangeness production**
 - Perturbative QCD strangeness production rates**
 - Bulk observables at RHIC and LHC**
 - Soft strange hadrons at LHC**
- [IV] **Where we are**

TWO ROOTS OF RELATIVISTIC HEAVY ION PROGRAM

STRUCTURED VACUUM – ORIGIN OF MASS:

Melt the vacuum structure and demonstrate mobility of quarks – ‘**deconfinement**’ – vacuum state determines what fundamental laws prevail in nature. The **confining vacuum** state is the origin of 99.9% of the rest mass present in the Universe.

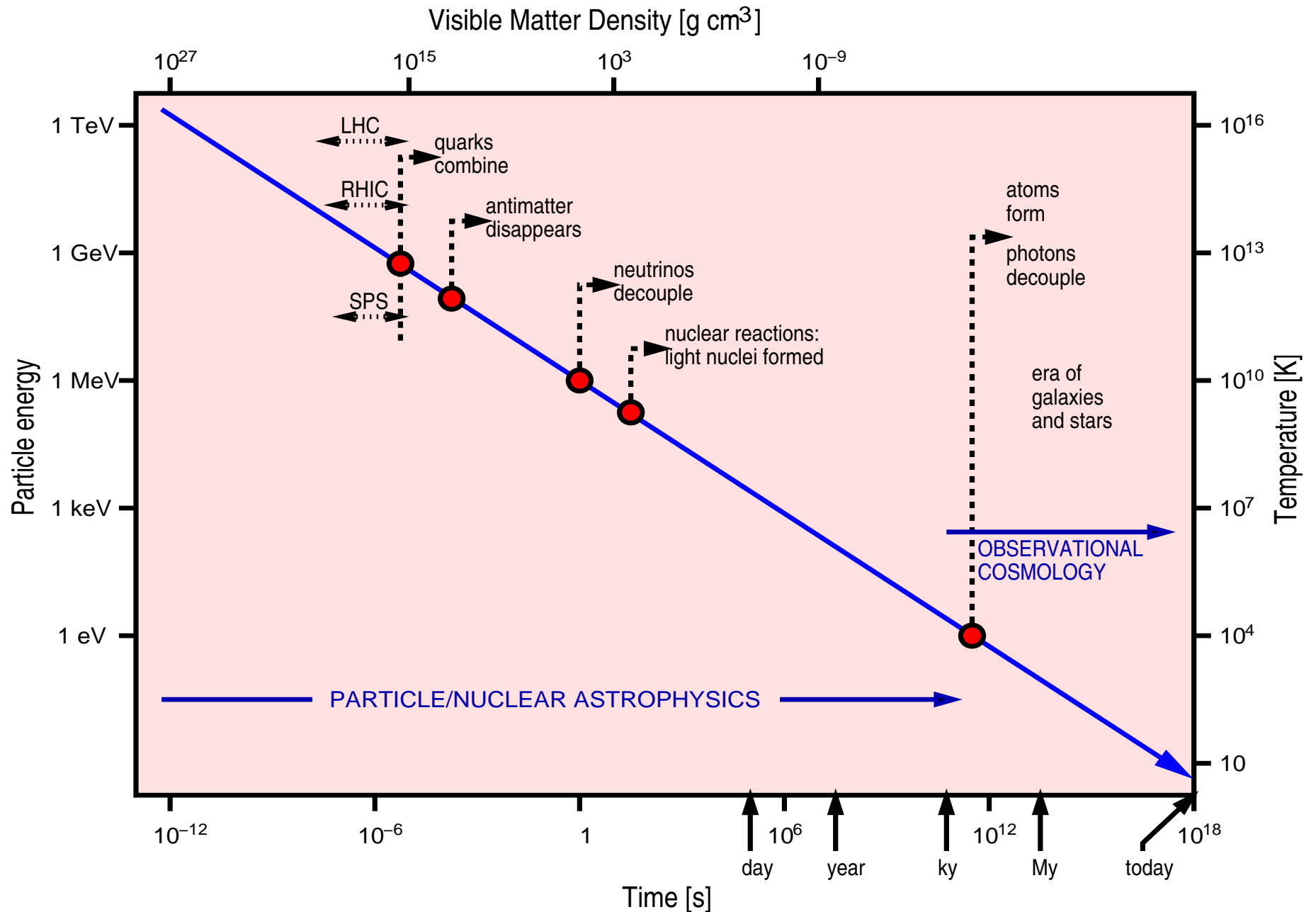
The celebrated Higgs mechanism covers the remaining 0.1% .

RECREATE THE EARLY UNIVERSE IN LABORATORY:

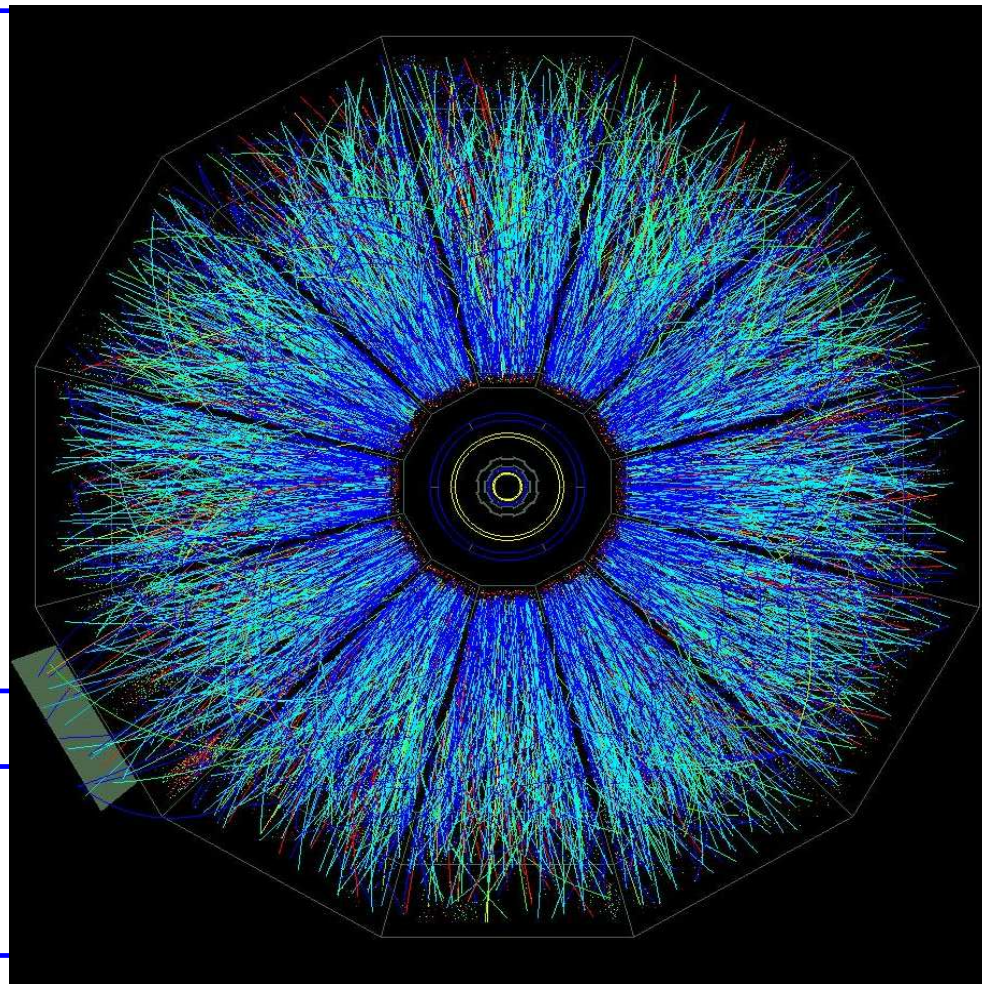
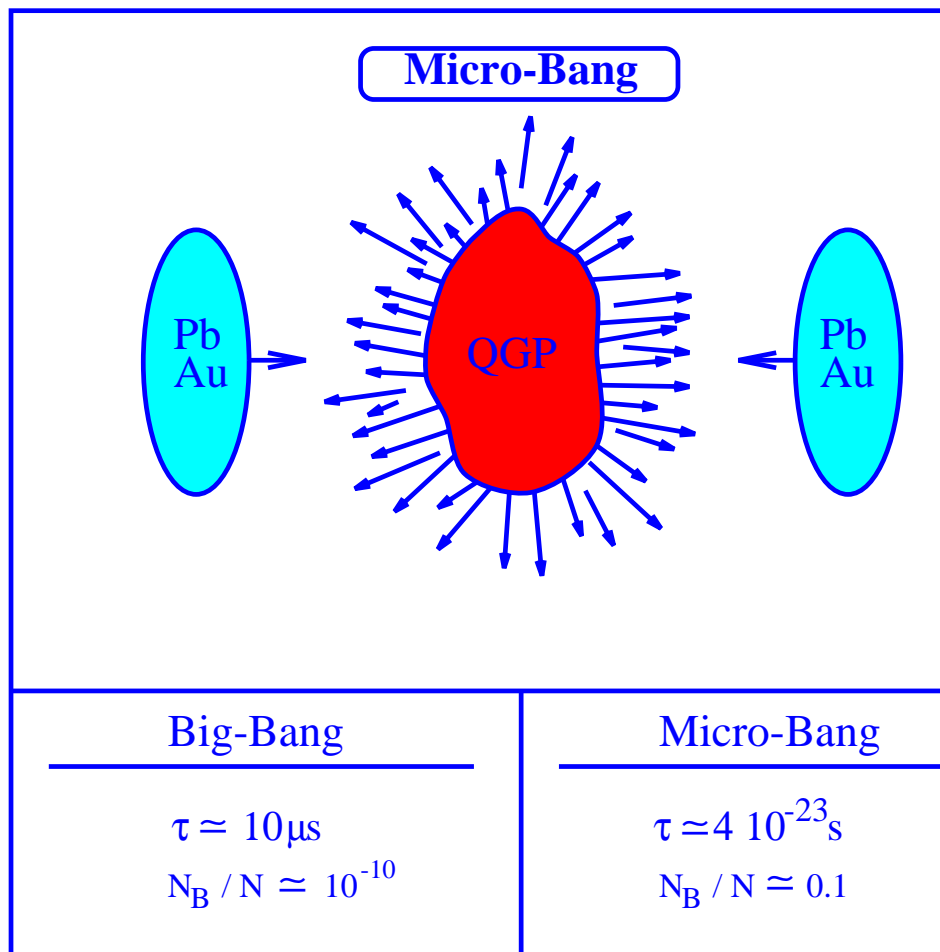
Recreate and understand the high energy density conditions prevailing in the Universe when **matter formed** from elementary degrees of freedom (quarks, gluons) **at about 30 μ s** after big bang.

Hadronization of the Universe led to nearly matter-antimatter symmetric state, the sequel annihilation left the small 10^{-10} matter asymmetry, the world around us.

Stages in the evolution of the Universe



RECREATING THE EARLY UNIVERSE IN LABORATORY



STAR at RHIC

Orders of Magnitude

ENERGY density	ϵ	$\simeq 1\text{--}50\text{GeV}/\text{fm}^3 = 0.18\text{--}9 \cdot 10^{16}\text{g}/\text{cc}$
Latent vacuum heat	B	$\simeq 0.1\text{--}0.4\text{GeV}/\text{fm}^3 \simeq (166\text{--}234\text{MeV})^4$
PRESSURE	P	$= \frac{1}{3}\epsilon = (0.52 - 26) \cdot 10^{30} \text{ barn}$
TEMPERATURE	T_0, T_f	700–250, 175–145 MeV; 300MeV \simeq 3.5 $\cdot 10^{12}$K

Challenge: Diagnosis of QGP at 10^{-23} s scale

- Deep probes (dileptons and photons)
- J/Ψ
- Dynamics of quark matter flow
- Jet tomography
- Strangeness
- Strange Antibaryons

Strangeness: a popular laboratory QGP diagnostic tool

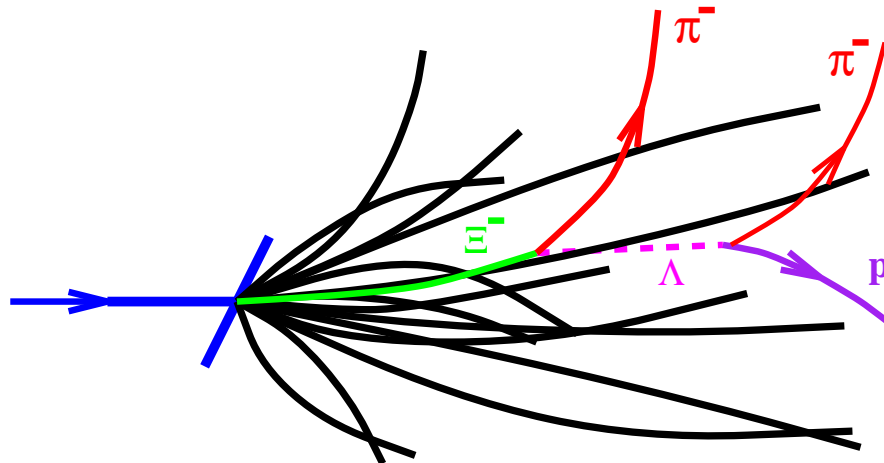
EXPERIMENTAL REASONS

- There are **many** strange particles allowing to study different physics questions ($q = u, d$):

$$\phi(s\bar{s}), \quad K(q\bar{s}), \quad \bar{K}(\bar{q}s), \quad \Lambda(qqs), \quad \bar{\Lambda}(\bar{q}\bar{q}\bar{s}),$$

$$\Xi(qss), \quad \bar{\Xi}(\bar{q}\bar{s}\bar{s}), \quad \Omega(sss), \quad \bar{\Omega}(\bar{s}\bar{s}\bar{s}) \quad \dots \text{resonances} \dots$$

- Strange hadrons are subject to a self analyzing decay within a few cm from the point of production;



- Production rates hence statistical significance is high;

THEORETICAL CONSIDERATIONS

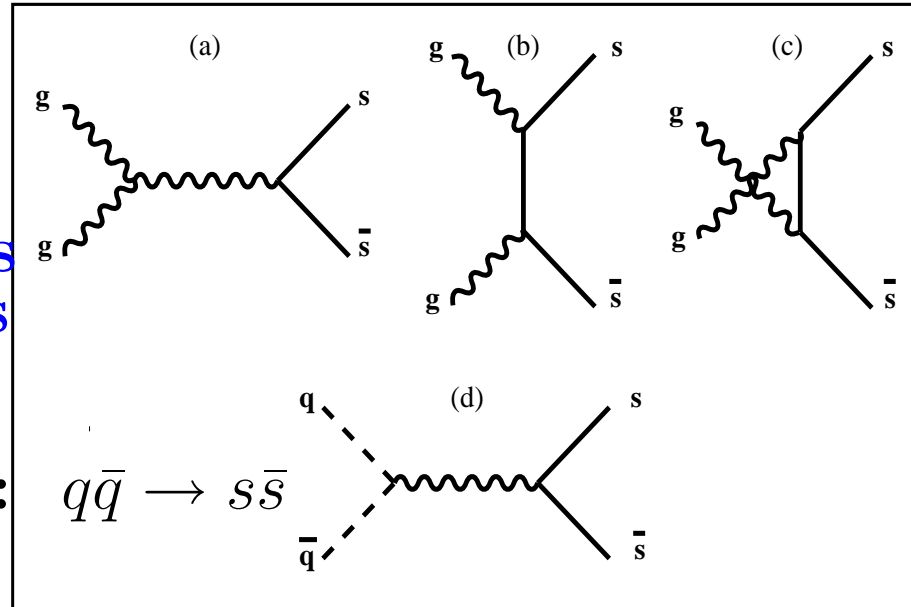
- production of strangeness in gluon fusion $GG \rightarrow s\bar{s}$
strangeness linked to gluons from QGP;

dominant processes:

$$GG \rightarrow s\bar{s}$$

abundant strangeness
=evidence for gluons

10–15% of total rate:



- coincidence of scales:

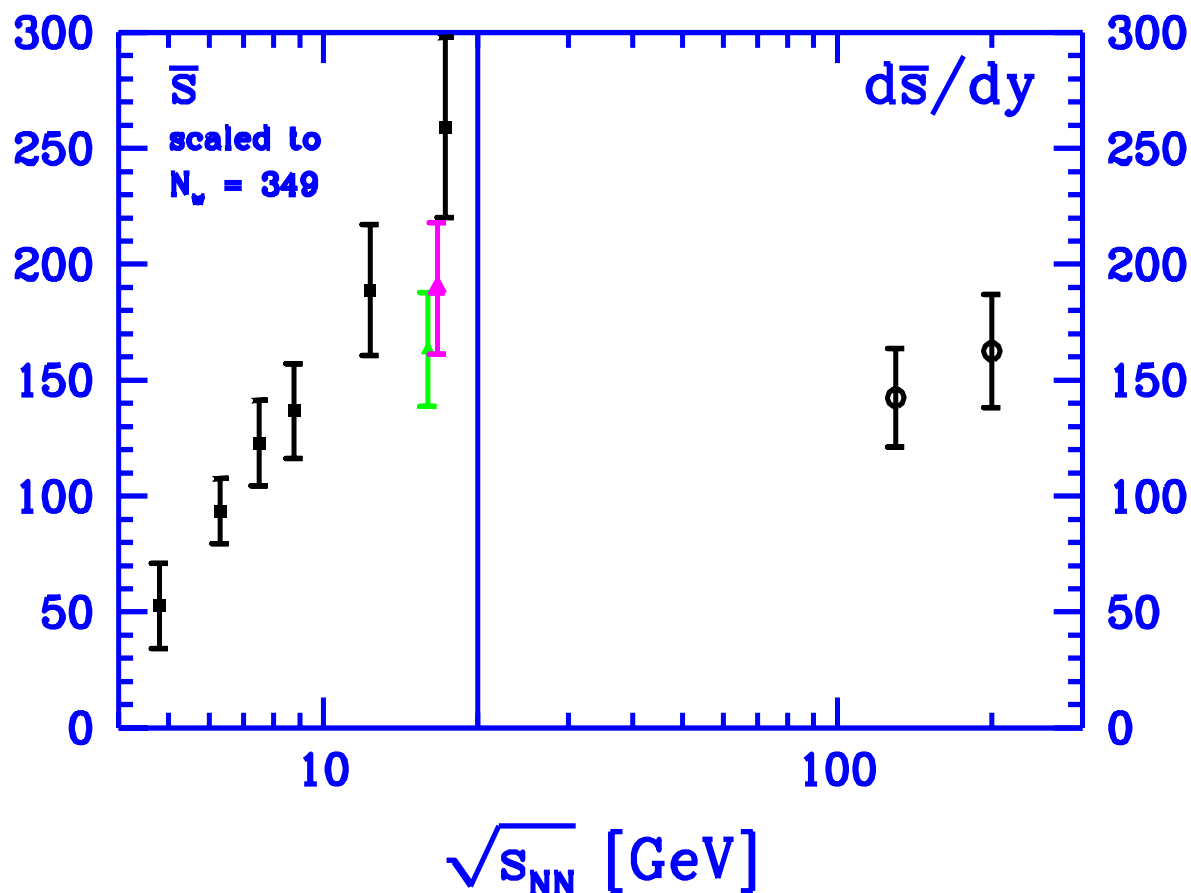
$$\boxed{m_s \simeq T_c} \rightarrow \boxed{\tau_s \simeq \tau_{\text{QGP}}} \rightarrow$$

clock for QGP phase

strangeness chemical equilibration in QGP possible

- $\bar{s} \simeq \bar{q}$ \rightarrow strange antibaryon enhancement
at RHIC (anti)hyperon dominance of (anti)baryons.

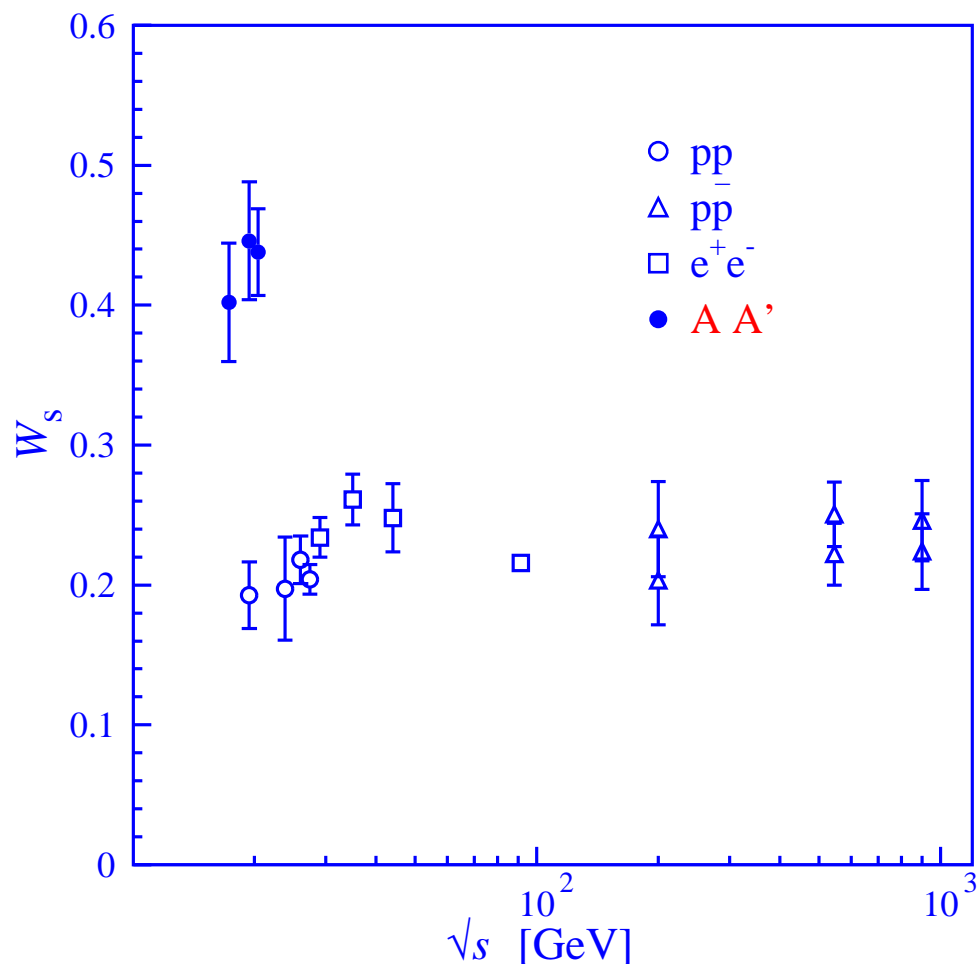
STRANGENESS EXCITATION FUNCTION



Green: C-C and Violet: Si-Si, other Au-Au, Pb-Pb Count \bar{s} quarks in all hadrons. At low energy practically $2K^+$.

No change in reaction mechanism visible, neither as function of energy, nor reaction volume, in this simple yield observable.

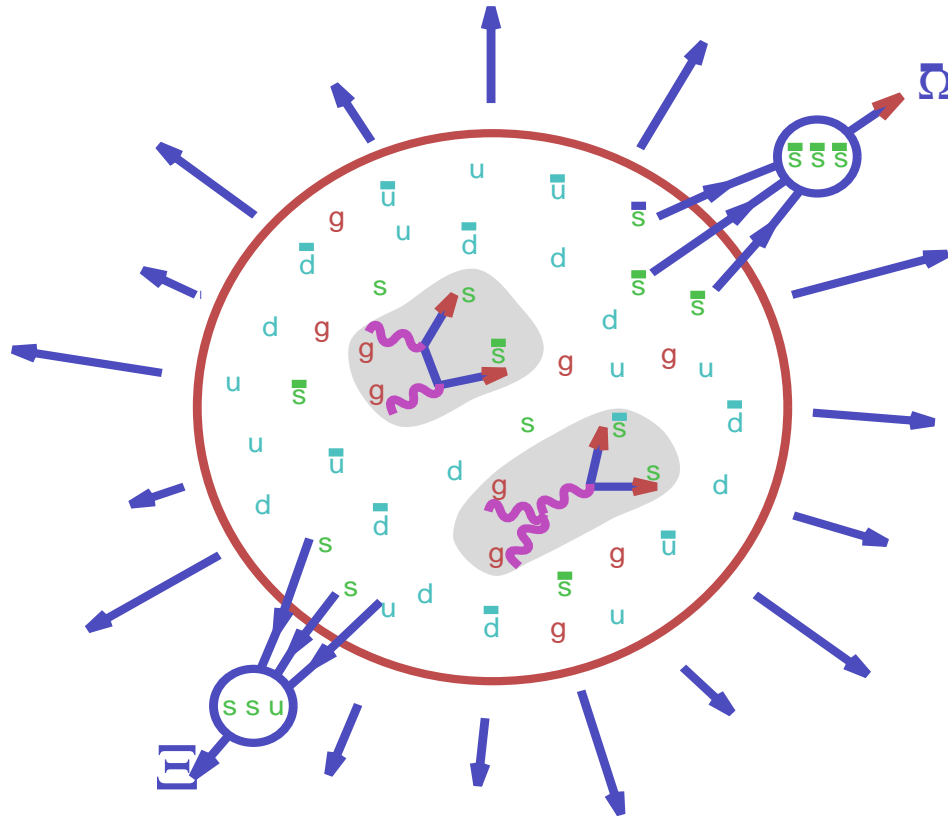
MORE EFFECTIVE CONVERSION OF ENERGY INTO STRANGENESS



Enhancement of strangeness pair production compared to light quarks due to onset of thermal glue fusion processes – seen most clearly in Wróblewski ratio in which only newly made s - and q -pairs are counted:

$$W = \frac{2\langle s\bar{s} \rangle}{\langle d\bar{d} + u\bar{u} \rangle}$$

TWO STEP HADRON FORMATION MECHANISM IN QGP



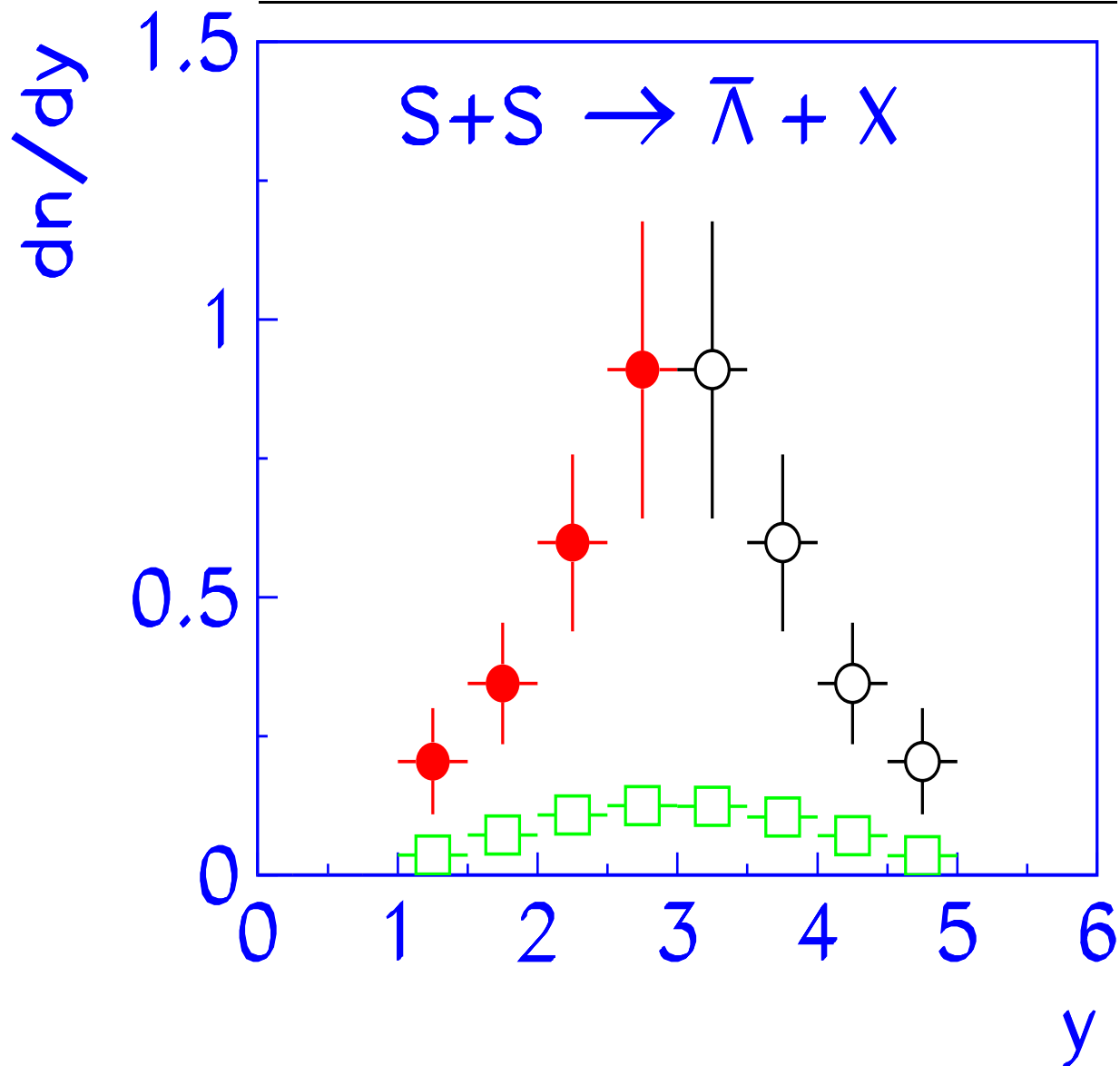
1. $GG \rightarrow s\bar{s}$ (thermal gluons collide)
 $GG \rightarrow c\bar{c}$ (initial parton collision)
 $GG \rightarrow b\bar{b}$ (initial parton collision)
gluon dominated reactions

2. hadronization of pre-formed
 $s, \bar{s}, c, \bar{c}, b, \bar{b}$ quarks

Formation of complex rarely produced (multi)exotic flavor (anti)particles from QGP **enabled by coalescence** between $s, \bar{s}, c, \bar{c}, b, \bar{b}$ quarks made in different microscopic reactions; **this is signature of quark mobility and independent action, thus of deconfinement.** Enhancement of flavored (strange, charm,...) antibaryons progressing with 'exotic' flavor content.

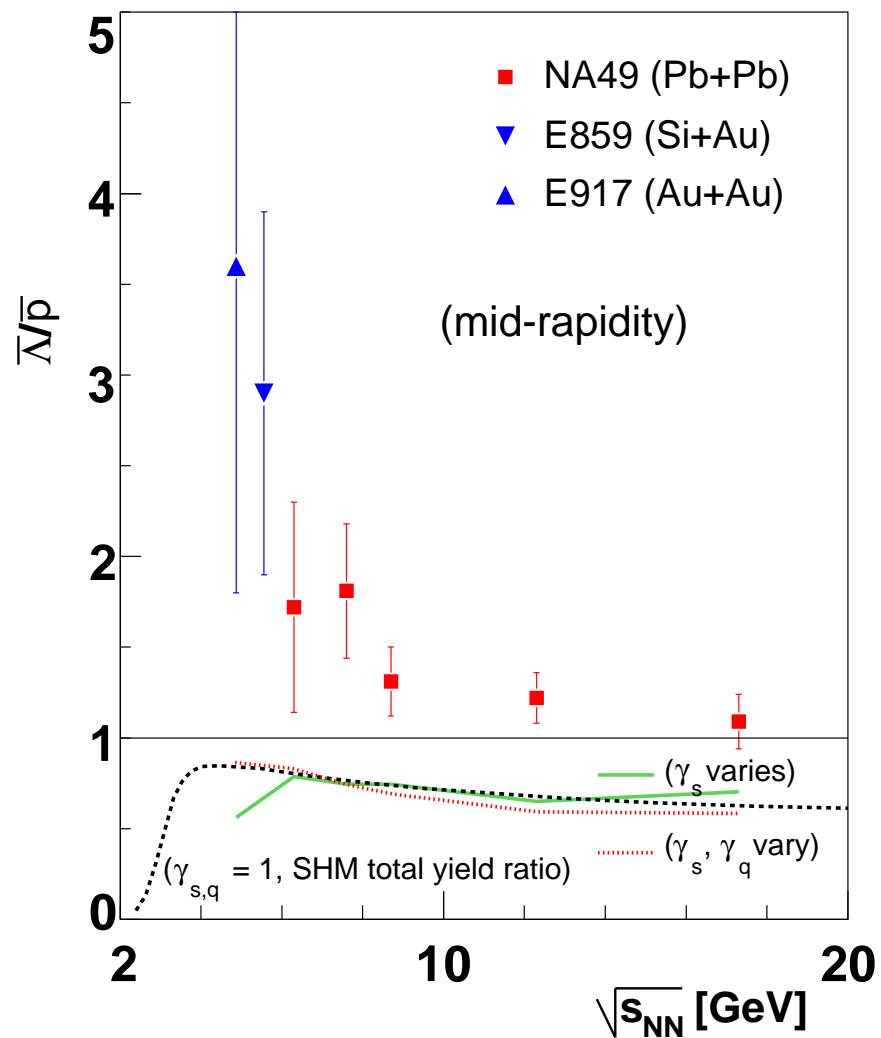
Retrospective: Strangeness Discoveries

Antibaryon excess at central CM rapidity



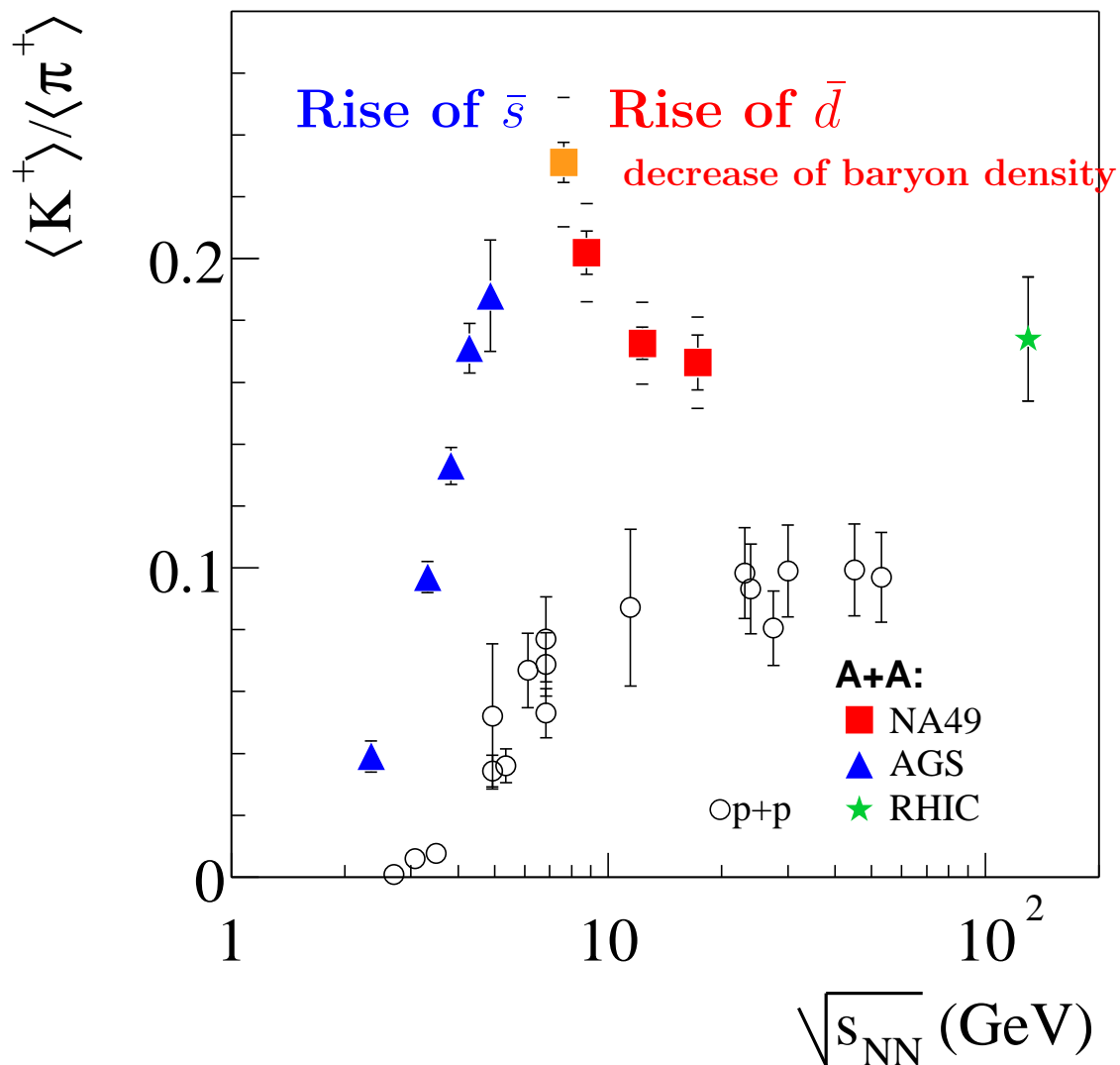
FIRST key result, 1990, SPS-NA35II EXCESS $\bar{\Lambda}$ emitted from a central well localized source. Background (squares) from multiplicity scaled NN reactions

Today systematic confirm of $\bar{\Lambda}/\bar{p} > 1$

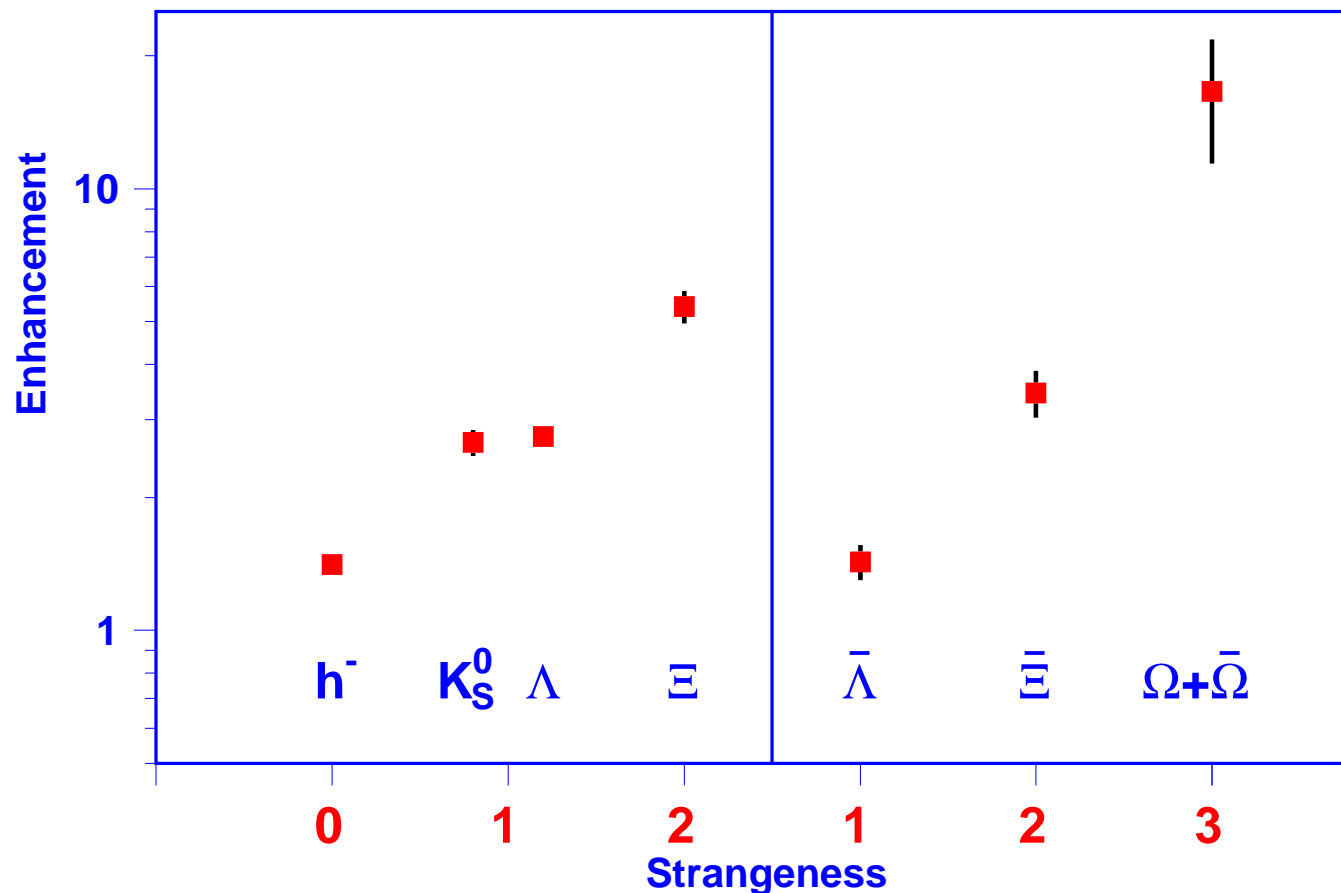


Results of CERN NA49 collaboration (M. Mitrovski), SQM2006

SPECTACULAR HORN

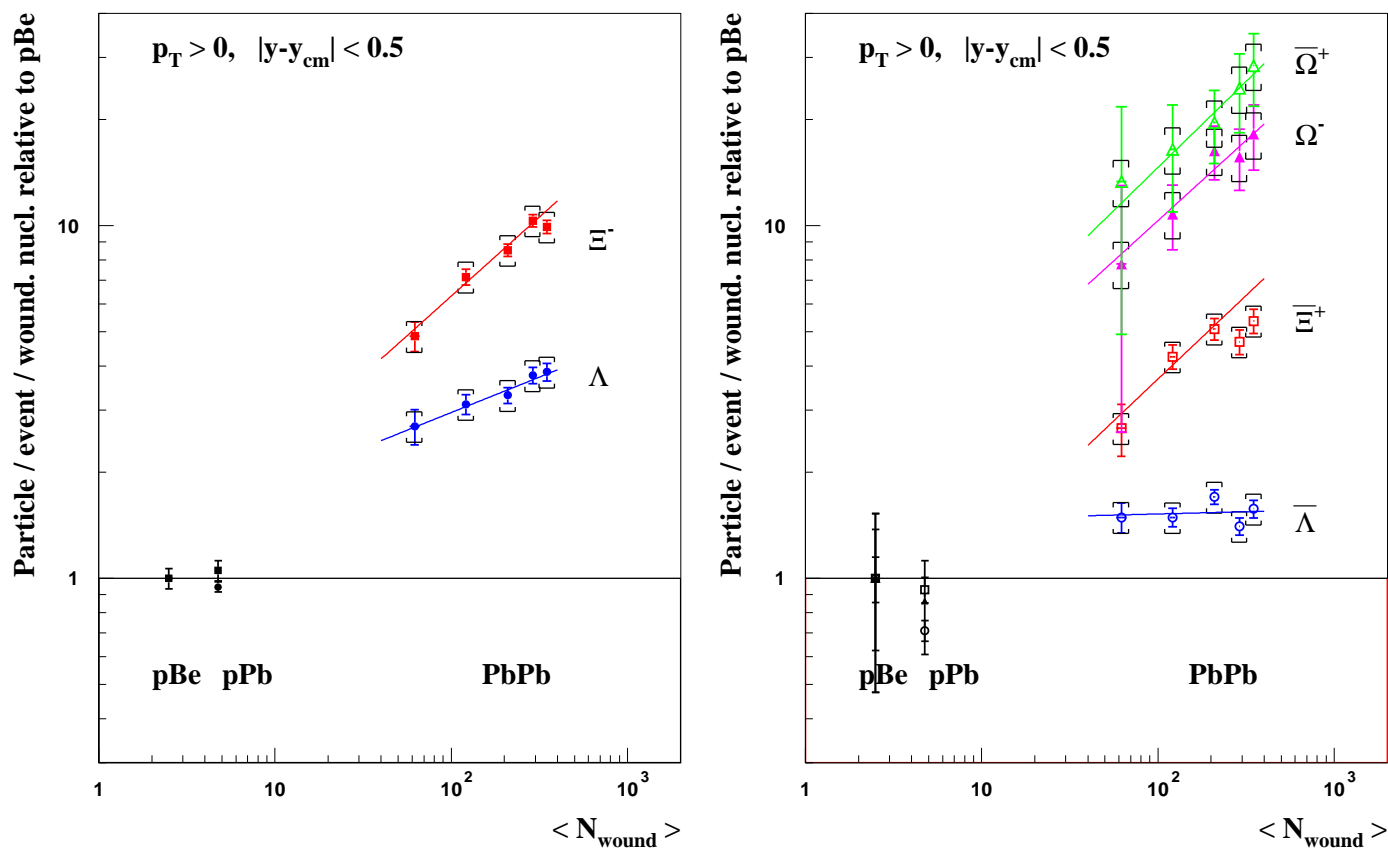


MULTI STRANGE HYPERON ENHANCEMENT



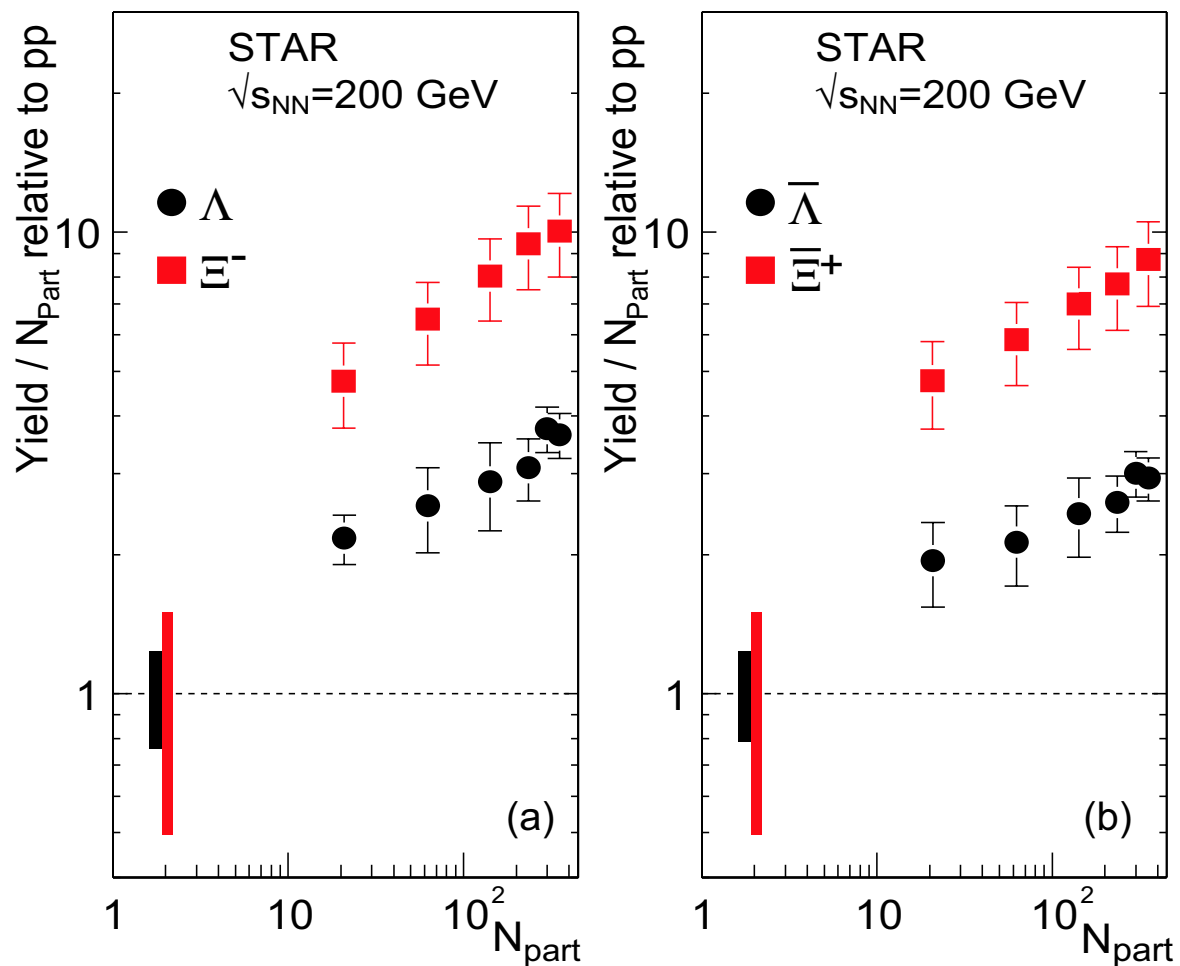
Results of CERN WA97/NA57 collaboration. Enhancement GROWS with a) strangeness b) antiquark content as predicted. Enhancement is defined with respect to yield in p-Be collisions, scaled up with the number of 'wounded' nucleons.

SPS MULTI STRANGE HYPERON ENHANCEMENT



Results of NA57 collaboration as function of centrality.

RHIC MULTI STRANGE HYPERON ENHANCEMENT



Results of the STAR collaboration. More available.

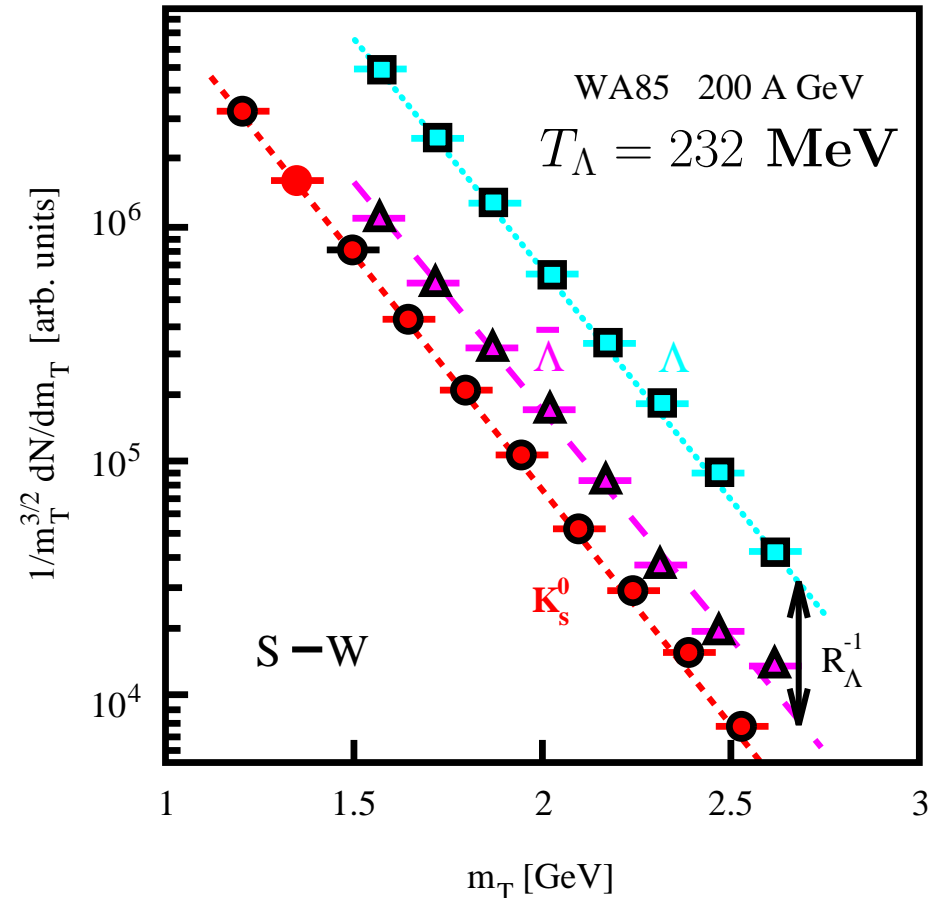
High m_{\perp} slope universality

Discovered in S-induced collisions, very pronounced in Pb-Pb Interactions.

Why is the slope of baryons and antibaryons precisely the same?

Why is the slope of different particles in same m_t range the same?

Analysis+Hypothesis 1991:
QGP quarks coalescing in SUDDEN hadronization



This allows to study ratios of particles measured only in a fraction of phase space

WA97	T_{\perp}^{Pb} [MeV]
T^{K^0}	230 ± 2
T^{Λ}	289 ± 3
$T^{\bar{\Lambda}}$	287 ± 4
T^{Ξ}	286 ± 9
$T^{\bar{\Xi}}$	284 ± 17
$T^{\Omega+\bar{\Omega}}$	251 ± 19

Λ within 1% of $\bar{\Lambda}$

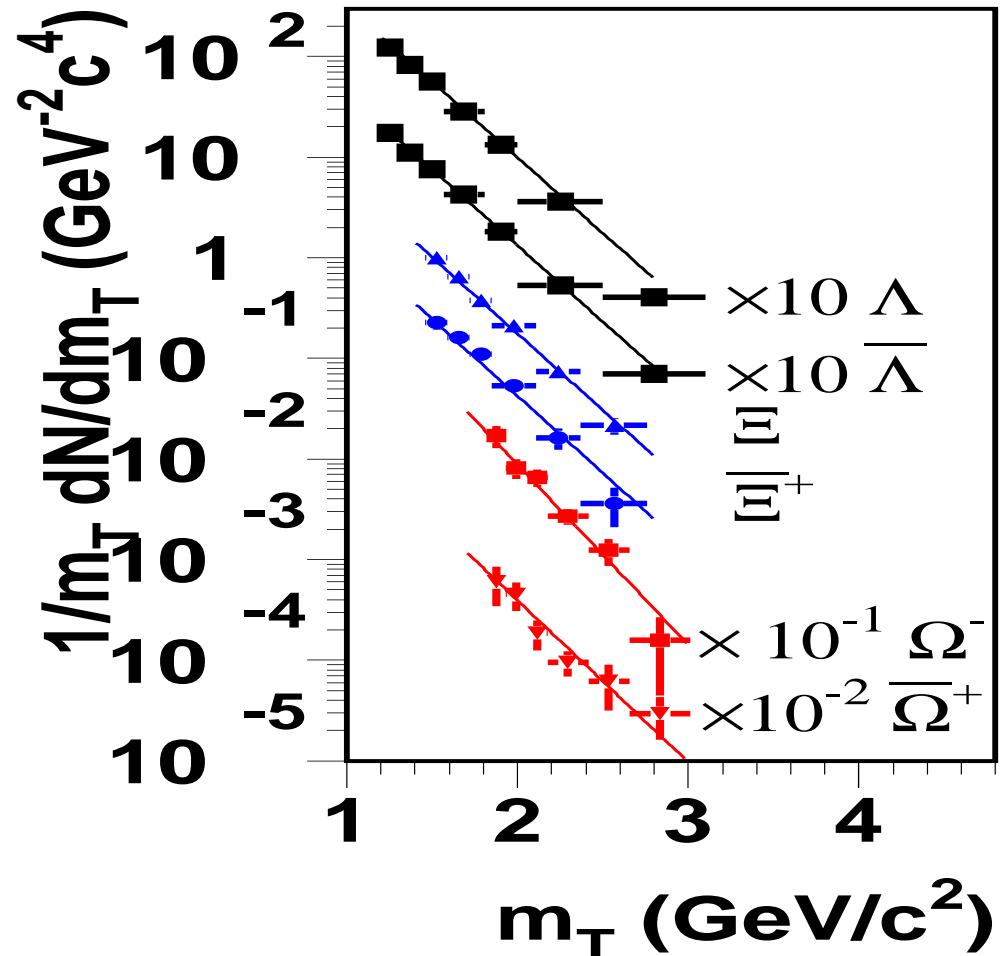
Kaon – hyperon difference:

EXPLOSIVE FLOW effect

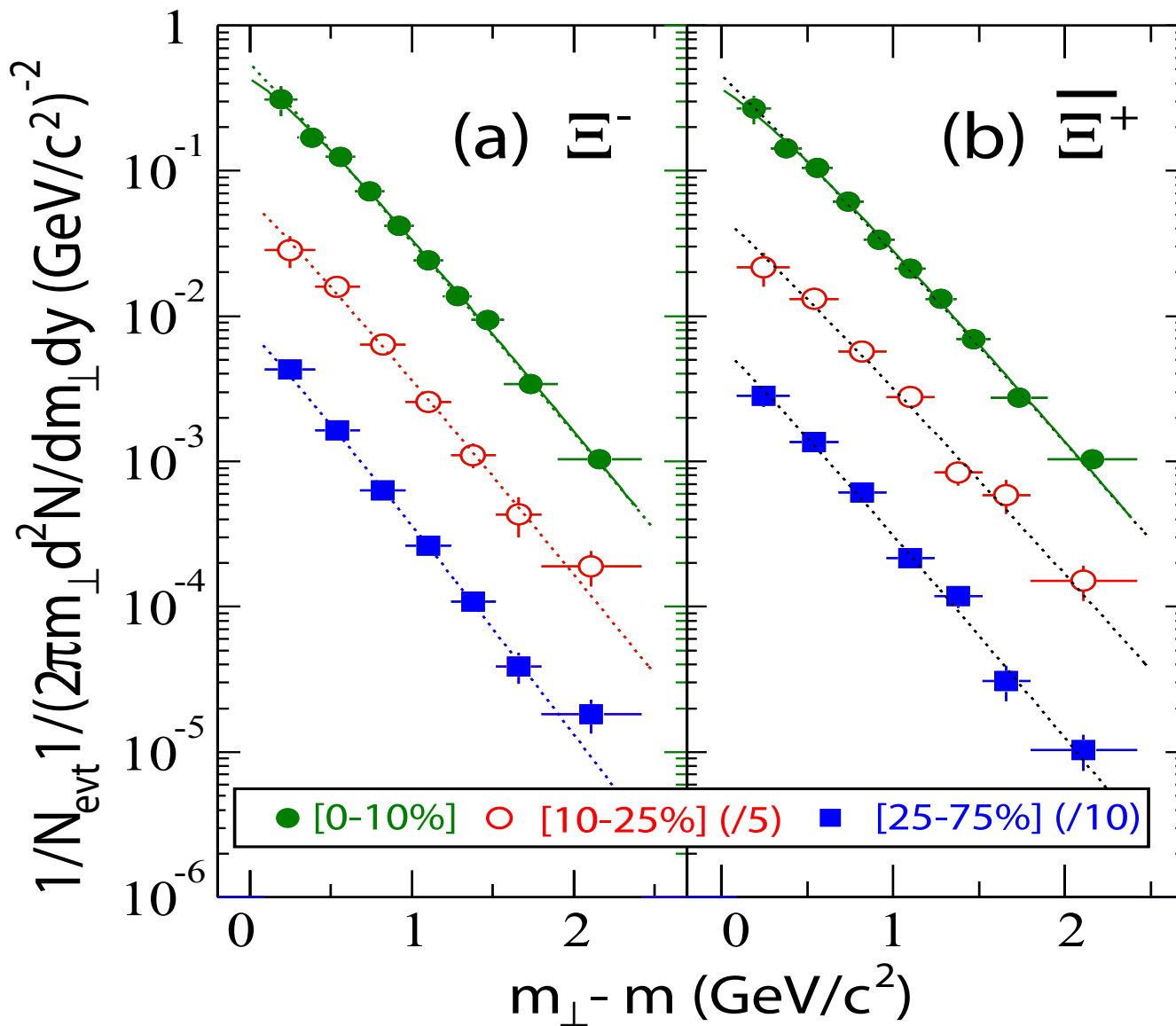
Difference between $\Omega + \bar{\Omega}$:

presence of an excess of low p_{\perp} particles

we will return to study this in spectral analysis



$\Xi^-, \bar{\Xi}^-$ Spectra RHIC-STAR 130+130 A GeV



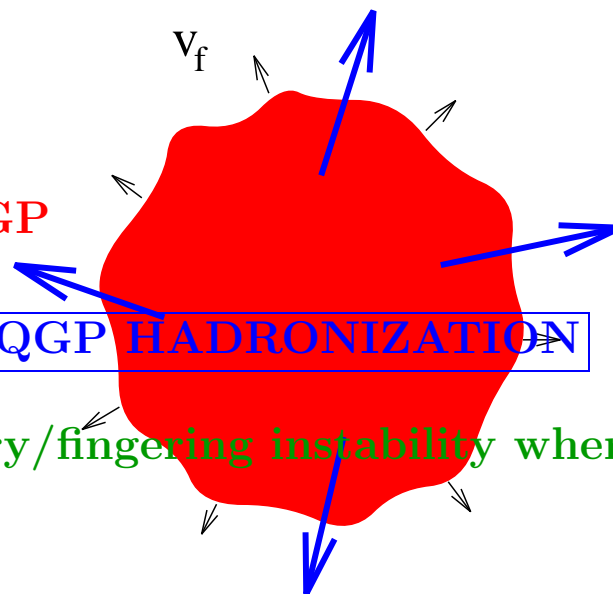
MATTER-ANTIMATTER PRODUCTION SYMMETRY

For the past 15 years experiments demonstrate **symmetry of m_{\perp} spectra of strange baryons and antibaryons in baryon rich environment.**

Interpretation: **Common matter-antimatter particle formation mechanism, little antibaryon re-annihilation in sequel evolution.**

Appears to be **free-streaming particle emission by a quark source into vacuum.** Such fast hadronization confirmed by other observables: e.g. reconstructed yield of hadron resonances. Note: within HBT particle correlation analysis: nearly same size pion source at all energies

Practically no hadronic 'phase'!
No 'mixed phase' either!
Direct emission of free-streaming hadrons from **exploding filamentary QGP**

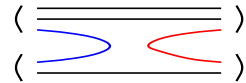
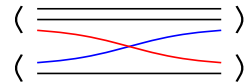


Develop analysis tools viable in **SUDDEN QGP HADRONIZATION**

Proposed reaction mechanism: **filamentary/fingering instability** when in expansion pressure reverses.

This implies chemical non-equilibrium of quark abundances

FOUR QUARKS: $s, \bar{s}, q, \bar{q} \rightarrow$ FOUR CHEMICAL PARAMETERS

γ_i controls overall abundance of quark ($i = q, s$) pairs	Absolute chemical equilibrium	HG production 
$\lambda_i = e^{\mu_i/T}$ controls difference between strange and light quarks ($i = q, s$)	Relative chemical equilibrium	HG exchange 

See Physics Reports 1986 Koch, Müller, JR

Boltzmann gas: $\gamma \equiv \frac{\rho(T, \mu)}{\rho^{\text{eq}}(T, \mu)}$

DISTINGUISH: hadron 'h' phase space and QGP phase parameters: micro-canonical variables such as baryon number, strangeness, charm, bottom, etc flavors are continuous, and entropy is almost continuous across phase boundary:

$$\gamma_s^{\text{QGP}} \rho_{\text{eq}}^{\text{QGP}} V^{\text{QGP}} = \gamma_s^{\text{h}} \rho_{\text{eq}}^{\text{h}} V^{\text{h}}$$

Equilibrium distributions are different in two phases and hence are densities:

$$\rho_{\text{eq}}^{\text{QGP}} = \int f_{\text{eq}}^{\text{QGP}}(p) dp \neq \rho_{\text{eq}}^{\text{h}} = \int f_{\text{eq}}^{\text{h}}(p) dp$$

Bulk strangeness as signature

1. TOTAL Strangeness YIELD: $s\text{strangeness}/S\text{entropy}$ depends primarily on **initial** conditions and **evolution** dynamics
(how long the system is at which T)
-

2. Strangeness at QGP BREAK-UP:

- a) $\gamma_s^{\text{QGP}} \rightarrow 1$ is QGP near chemical equilibrium?

$$\gamma_{s,q}^{\text{QGP}} = \frac{n_{s,q}(t, T(t))}{n_{s,q}(\infty, T(t))} \Big|_{\text{QGP}} \rightarrow 1?$$

- b) $\gamma_s^{\text{HG}} \simeq 3\gamma_s^{\text{QGP}}$ QGP phase space is squeezed into a smaller number of HG phase space cells
-

- 2'. TO BE SENSITIVE WE NEED ALSO TO CONSIDER $\gamma_q^{\text{HG}} > 1$
over population of pion phase space is ENTROPY enhancement
-

3. STRANGENESS MOBILITY IN QGP IMPLIES
 $s-\bar{s}$ phase space symmetry, relevant in baryon rich (SPS) environment
 $\lambda_s^{\text{eff}} = 1$ IMPRINTED ON HADRONS AT HADRONIZATION

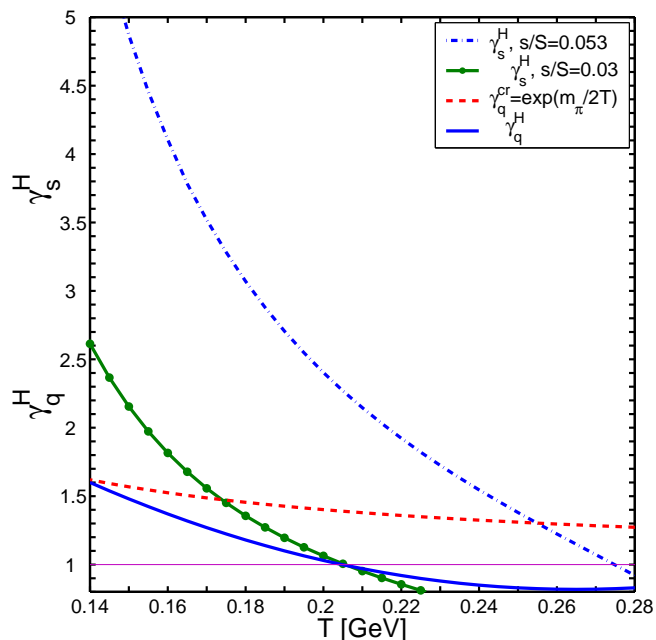
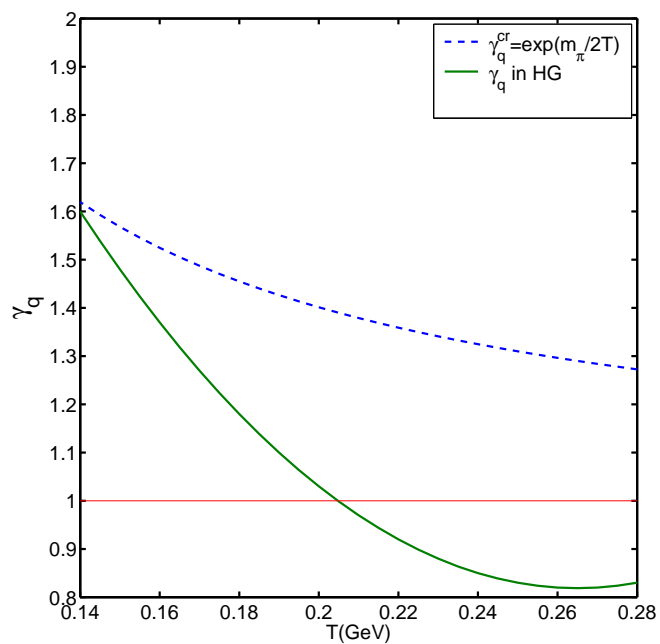
Smooth across the phase boundary are the yields
 strangeness, charm, entropy = multiplicity
 and hence ratios, we will be interested in the observables such as:

$$\frac{s \text{ or } c}{S} = \frac{\text{number of valance strange, charm quark pairs}}{\text{multiplicity} = \text{entropy content in final state}}$$

And across any phase boundary when V does not adjust (and even in that case)

$$\gamma_s^{\text{QGP}} \neq \gamma_s^{\text{h}} \quad \gamma_q^{\text{QGP}} \neq \gamma_q^{\text{h}}$$

QGP in chem equilibrium to hadron breakup at fixed V , S , and s



Counting hadronic particles

The counting of hadrons is conveniently done by counting the valence quark content ($u, d, s, \dots \lambda_q^2 = \lambda_u \lambda_d, \lambda_{I3} = \lambda_u / \lambda_d$) :

$$\Upsilon_i \equiv \prod_i \gamma_i^{n_i} \lambda_i^{k_i} = e^{\sigma_i/T}; \quad \lambda_q \equiv e^{\frac{\mu_q}{T}} = e^{\frac{\mu_b}{3T}}, \quad \lambda_s \equiv e^{\frac{\mu_s}{T}} = e^{\frac{[\mu_b/3 - \mu_s]}{T}}$$

Example of NUCLEONS $\gamma_N = \gamma_q^3$:

$$\Upsilon_N = \gamma_N e^{\frac{\mu_b}{T}}, \quad \Upsilon_{\bar{N}} = \gamma_N e^{\frac{-\mu_b}{T}};$$

$$\sigma_N \equiv \mu_b + T \ln \gamma_N, \quad \sigma_{\bar{N}} \equiv -\mu_b + T \ln \gamma_N$$

Meaning of parameters from e.g. the first law of thermodynamics:

$$\begin{aligned} dE + P dV - T dS &= \sigma_N dN + \sigma_{\bar{N}} d\bar{N} \\ &= \mu_b (dN - d\bar{N}) + T \ln \gamma_N (dN + d\bar{N}). \end{aligned}$$

NOTE: For $\gamma_N \rightarrow 1$ the pair terms vanishes, the μ_b term remains, it costs $dE = \mu_B$ to add to baryon number.

HIGH ENTROPY STATE AND THE EXPECTED γ_q^{HG}

QGP has excess of entropy, maximize entropy density at hadronization:

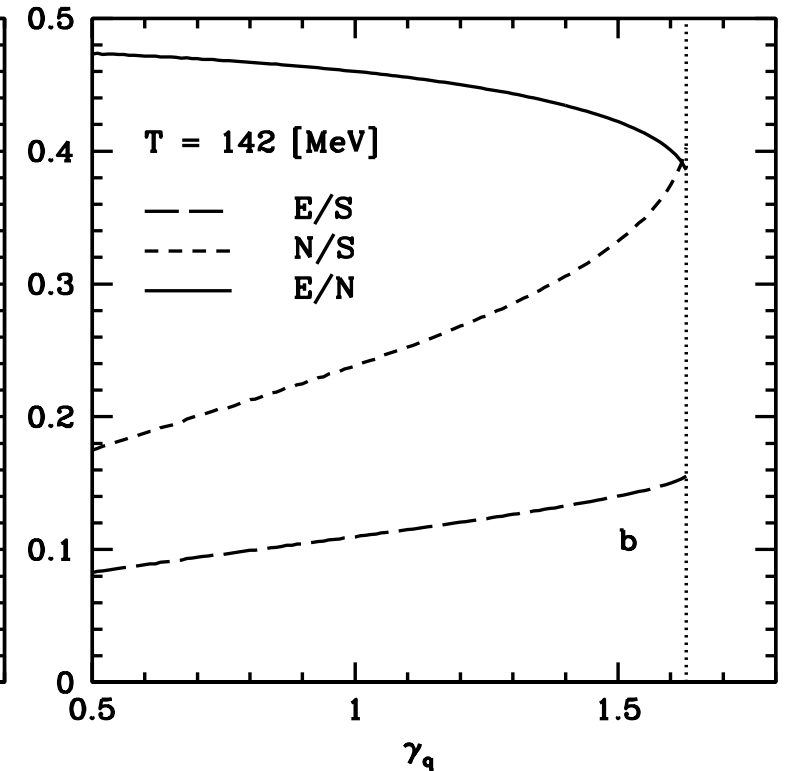
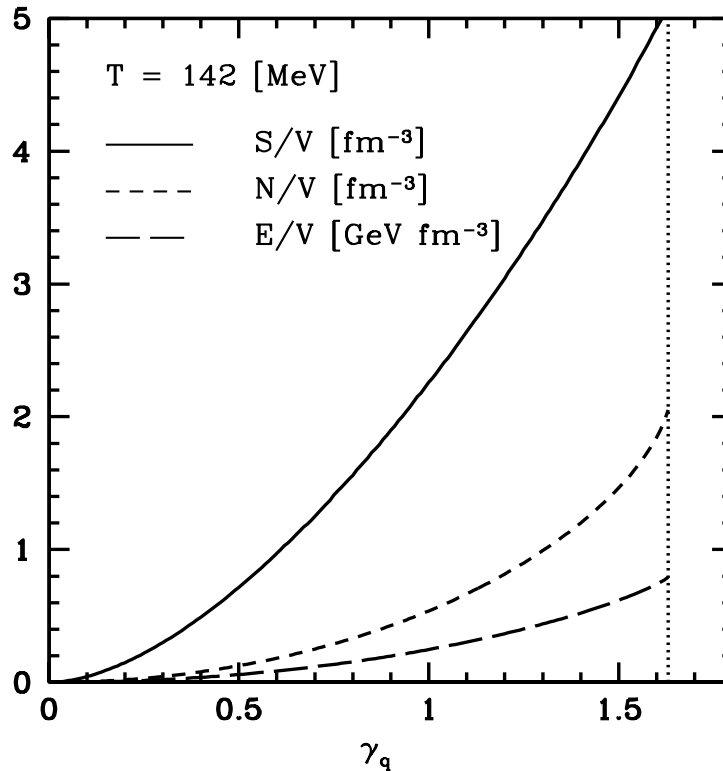
$$\gamma_q^2 \rightarrow e^{m_\pi/T} :$$

Example: maximization of entropy density in pion gas

$$E_\pi = \sqrt{m_\pi^2 + p^2}$$

$$S_{B,F} = \int \frac{d^3p d^3x}{(2\pi\hbar)^3} [\pm(1 \pm f) \ln(1 \pm f) - f \ln f] , \quad f_\pi(E) = \frac{1}{\gamma_q^{-2} e^{E_\pi/T} - 1} .$$

Pion gas properties:
N-particle,
E-energy,
S-entropy,
V-volume
 as function
 of γ_q .



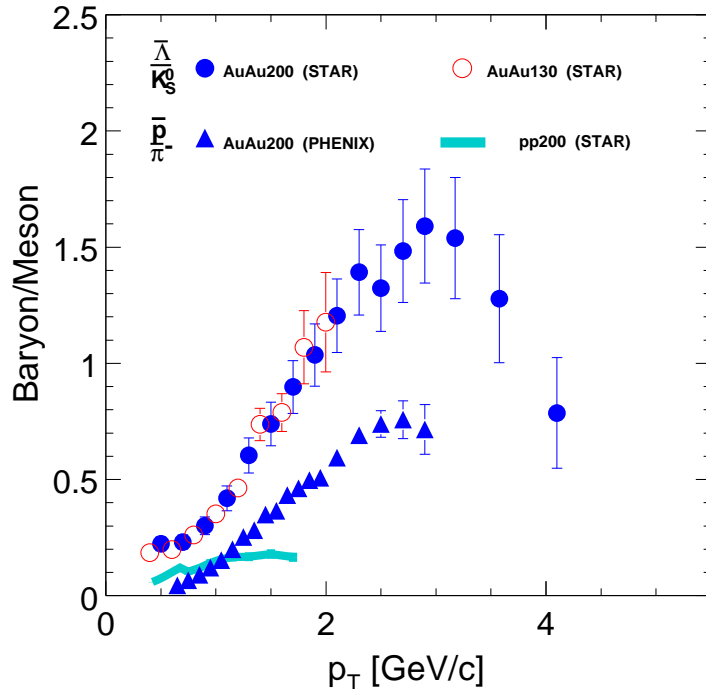
Physical Impact of Non-Equilibrium Parameters

- $\tilde{\gamma}_s \equiv \gamma_s/\gamma_q$ shifts the yield of strange vs non-strange hadrons:

$$\frac{K^+(u\bar{s})}{\pi^+(u\bar{d})} \propto \frac{\gamma_s}{\gamma_q}, \quad \frac{\phi}{h} \propto \frac{\gamma_s^2}{\gamma_q^2}, \quad \frac{\Omega(sss)}{\Lambda(sud)} \propto \frac{\gamma_s^2}{\gamma_q^2},$$

- For fixed $\tilde{\gamma}_s \equiv \gamma_s/\gamma_q$ and fixed other statistical parameters (T, λ_i, \dots):

$$\frac{\text{baryons}}{\text{mesons}} \propto \frac{\gamma_q^3}{\gamma_q^2} = \gamma_q.$$



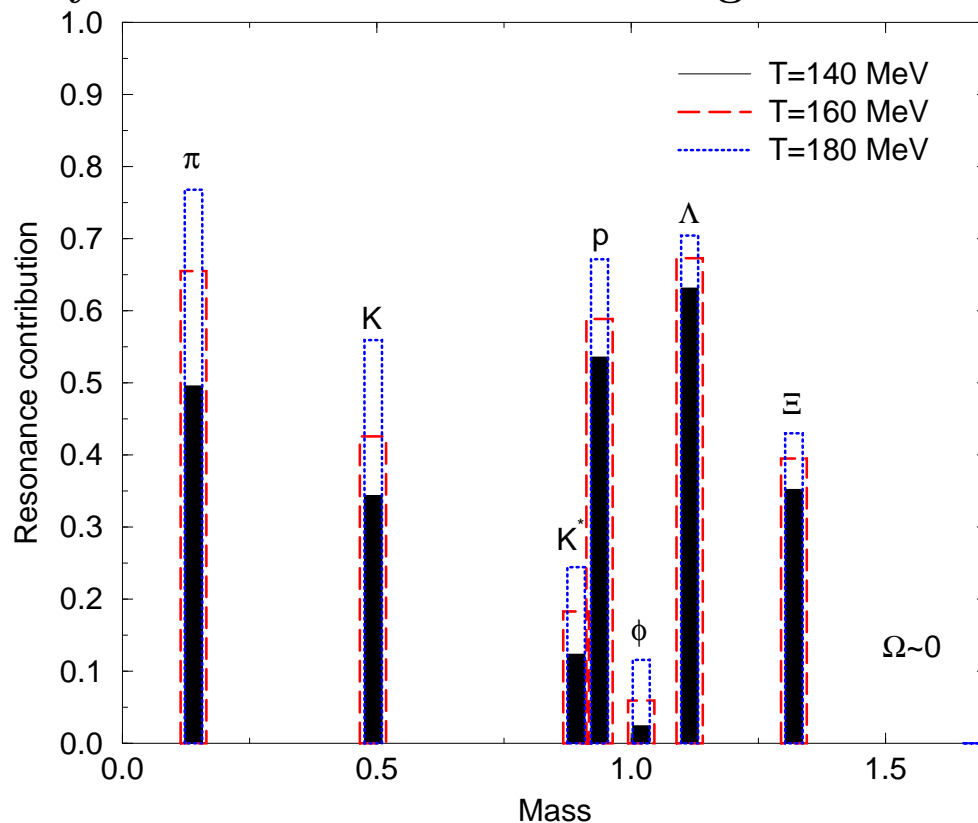
Ratios of $\bar{\Lambda}$ to K_S from AuAu and pp collisions (STAR) and \bar{p} to π from AuAu collisions (PHENIX) as a function of transverse momentum (p_\perp). The large ratio at the intermediate p_\perp region: evidence that particle formation at RHIC distinctly different from fragmentation processes for the elementary e^+e^- and nucleon-nucleon collisions.

STATISTICAL HADRONIZATION

Hypothesis (**Fermi, Hagedorn**): particle production can be described by evaluating the accessible phase space.

Verification of statistical hadronization:

Particle yields with same valance quark content are in relative chemical equilibrium, e.g. the relative yield of $\Delta(1230)/N$ as of K^*/K , $\Sigma^*(1385)/\Lambda$, etc, is controlled by chemical freeze-out i.e. Hagedorn Temperature T_H :



$$\frac{N^*}{N} = \frac{g^*(m^*T_H)^{3/2}e^{-m^*/T_H}}{g(mT_H)^{3/2}e^{-m/T_H}}$$

Resonances decay rapidly into ‘stable’ hadrons and dominate the yield of most stable hadronic particles.

Resonance yields test statistical hadronization principles.

Resonances reconstructed by invariant mass; important to consider potential for loss of observability.

HADRONIZATION GLOBAL FIT:→

OBSERVABLE RESONANCE YIELDS

Invariant mass method: construct invariant mass from decay products:

$$M^2 = (\sqrt{m_a^2 + \vec{p}_a^2} + \sqrt{m_b^2 + \vec{p}_b^2} + \dots)^2 - (\vec{p}_a + \vec{p}_b + \dots)^2$$

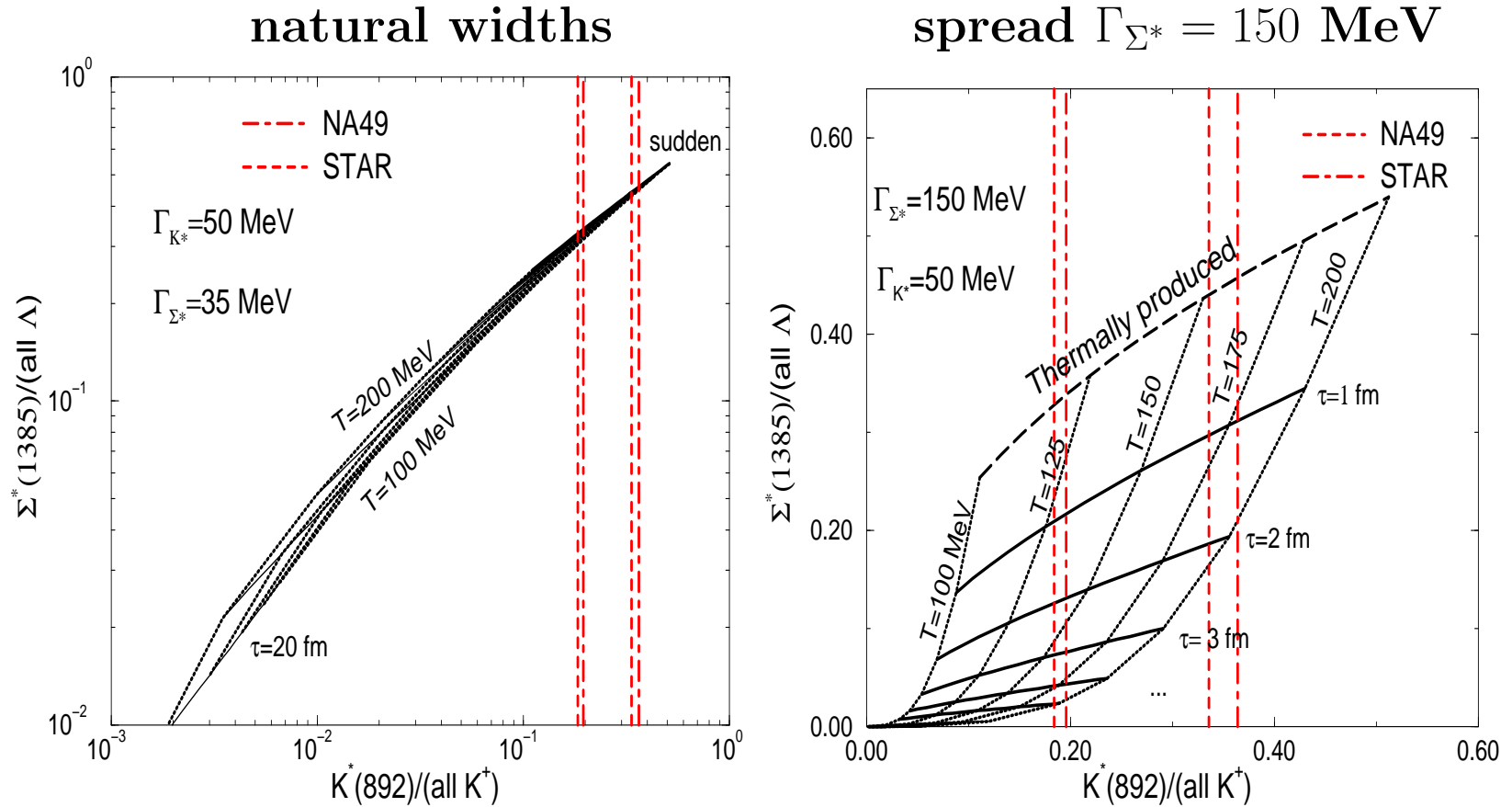
If one of decay products rescatter the reconstruction not assured.

Strongly interacting matter essentially non-transparent. Simplest model: If resonance decays $N^* \rightarrow D + \dots$ within matter, resonance can disappear from view. **Model implementation:**

$$\frac{dN^*}{dt} = -\Gamma N^* + R, \quad \frac{dD}{dt} = \Gamma N^*, \quad \frac{dN_{\text{rec}}^*}{dt} = \Gamma N^* - D \sum_j \langle \sigma_{Dj} v_{Dj} \rangle \rho_j(t)$$

To obtain the observable resonance yield N_{rec}^* we integrate to the time $t = \tau$ spend by N^* in the opaque matter, and add the remainder from free space decay. **Regeneration term $R \propto \langle \sigma_{Di}^{\text{INEL}} v_{Di} \rangle \rho_i$ negligible since production reactions very much weaker than total scattering.** Hadronic matter acts as black cloud, practically all in matter decays cannot be reconstructed.

TWO resonance ratios combined



Dependence of the combined $\Sigma^*/(\text{all } \Lambda)$ with $K^*(892)/(\text{all } K)$ signals on the chemical freeze-out temperature and HG phase lifetime.

Even the first rough measurement of K^*/K indicates that there is no long lived hadron phase. In matter widening makes this conclusion stronger.

Await forthcoming STAR Σ^* yields.

Statistical Hadronization fits of hadron yields

Full analysis of experimental hadron yield results requires a significant numerical effort in order to allow for resonances, particle widths, full decay trees, isospin multiplet sub-states.

Kraków-Tucson (and SHARE 2 Montreal) collaboration produced a public package **SHARE Statistical Hadronization with Resonances** which is available e.g. at

<http://www.physics.arizona.edu/~torrieri/SHARE/share.html>

Lead author: Giorgio Torrieri

GT, W. Broniowski, W. Florkowski, J. Letessier, S. Steinke, JR
nucl-th/0404083 Comp. Phys. Com. 167, 229 (2005)

SHARE 2 with flexible weak decays, fluctuations and chemical flexibility now on line and in review. Involves S.Y. Jeon, Montreal (of fluctuation fame)

Online SHARE1.2: Steve Steinke No fitting online (server too small)

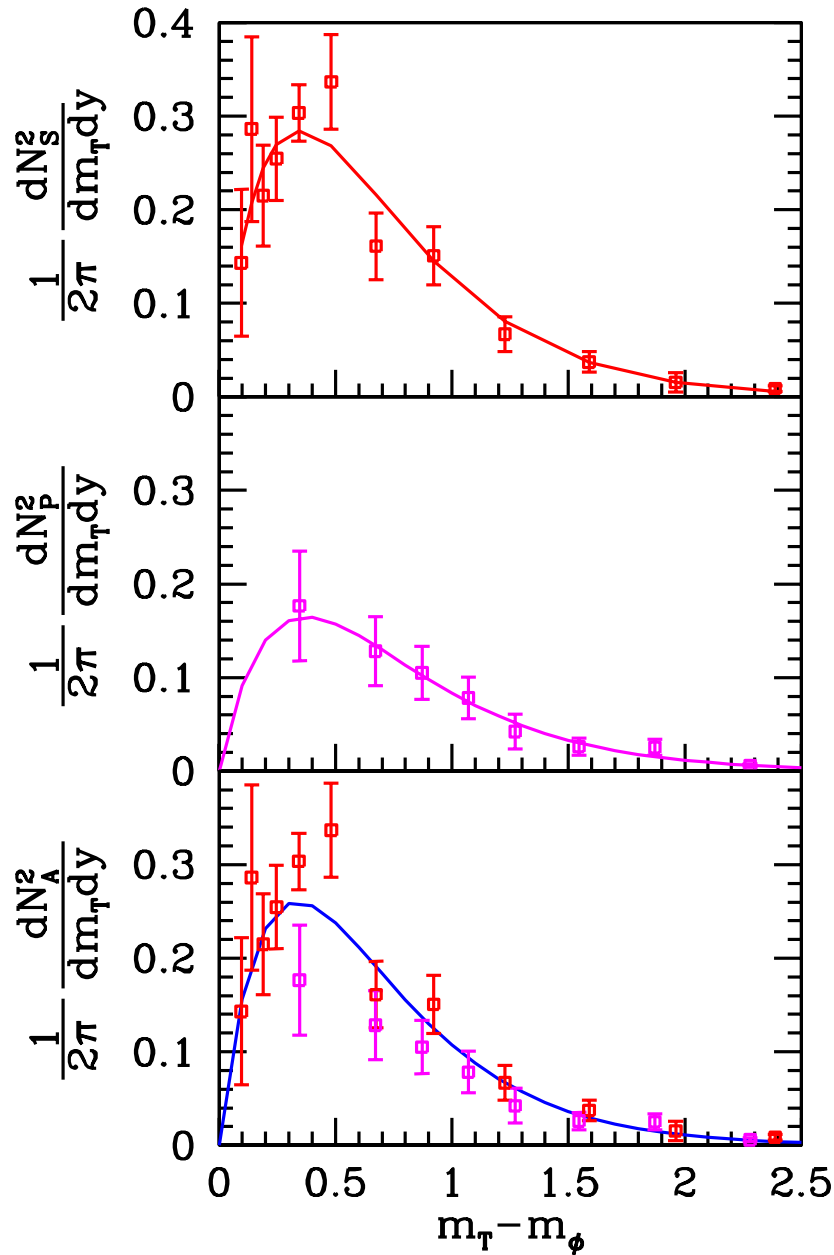
<http://www.physics.arizona.edu/~steinke/shareonline.html>

Aside of particle yields, also PHYSICAL PROPERTIES of the source are available, both in SHARE and ONLINE.

DATA: Centrality dependence of dN/dy for π^\pm , K^\pm , p and \bar{p} . The errors are systematic only. The statistical errors are negligible. PHENIX data

N_{part}	π^+	π^-	K^+	K^-	p	\bar{p}
351.4	286.4 ± 24.2	281.8 ± 22.8	48.9 ± 6.3	45.7 ± 5.2	18.4 ± 2.6	13.5 ± 1.8
299.0	239.6 ± 20.5	238.9 ± 19.8	40.1 ± 5.1	37.8 ± 4.3	15.3 ± 2.1	11.4 ± 1.5
253.9	204.6 ± 18.0	198.2 ± 16.7	33.7 ± 4.3	31.1 ± 3.5	12.8 ± 1.8	9.5 ± 1.3
215.3	173.8 ± 15.6	167.4 ± 14.4	27.9 ± 3.6	25.8 ± 2.9	10.6 ± 1.5	7.9 ± 1.1
166.6	130.3 ± 12.4	127.3 ± 11.6	20.6 ± 2.6	19.1 ± 2.2	8.1 ± 1.1	5.9 ± 0.8
114.2	87.0 ± 8.6	84.4 ± 8.0	13.2 ± 1.7	12.3 ± 1.4	5.3 ± 0.7	3.9 ± 0.5
74.4	54.9 ± 5.6	52.9 ± 5.2	8.0 ± 0.8	7.4 ± 0.6	3.2 ± 0.5	2.4 ± 0.3
45.5	32.4 ± 3.4	31.3 ± 3.1	4.5 ± 0.4	4.1 ± 0.4	1.8 ± 0.3	1.4 ± 0.2
25.7	17.0 ± 1.8	16.3 ± 1.6	2.2 ± 0.2	2.0 ± 0.1	0.93 ± 0.15	0.71 ± 0.12
13.4	7.9 ± 0.8	7.7 ± 0.7	0.89 ± 0.09	0.88 ± 0.09	0.40 ± 0.07	0.29 ± 0.05
6.3	4.0 ± 0.4	3.9 ± 0.3	0.44 ± 0.04	0.42 ± 0.04	0.21 ± 0.04	0.15 ± 0.02

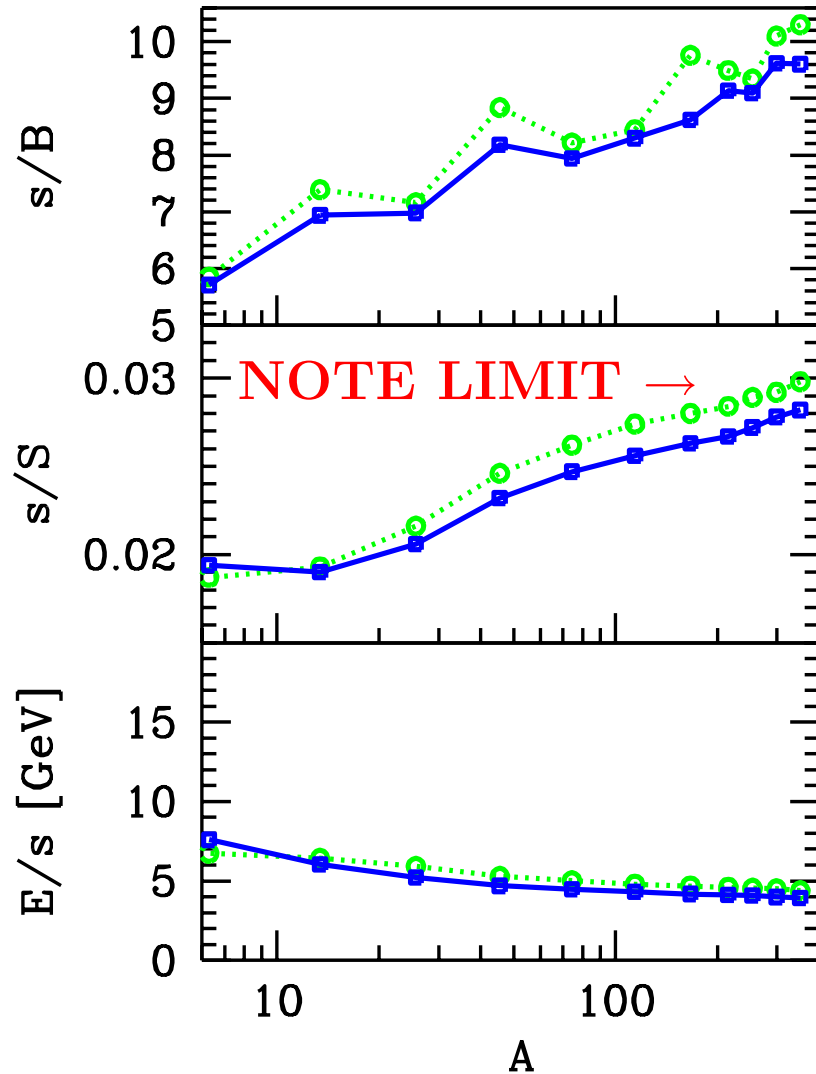
and STAR ϕ and K^* yields



Include STAR data on $K^*(892)/K^-$, and ϕ/K^- relative yields, these help decisively fix γ_s ($\phi \propto \gamma_s^2$) and $T : Y \propto m^{3/2} e^{-m/T}$ for $m \gg T$.

We considered the difference between STAR and PHENIX ϕ yields. The lines show our best fit results to STAR (top panel), PHENIX (middle panel) and combined data set (bottom panel). The integrated yields agree for the top two panels with those reported by the experimental collaborations. We note that the integrated yield derived from the combined data fit (bottom panel), to all available 10% centrality ϕ -yields, is not compatible with the PHENIX yield. This is so, since the evaluation of the integrated PHENIX ϕ -yield depends on the lowest m_\perp measured yield. This data point appears to be a 1.5 s.d. low anomaly compared to the many STAR ϕ -results available at low m_\perp . This possibly statistical fluctuation materially influences the total integrated PHENIX ϕ -yield.

s/b and s/S rise with increasing centrality $A \propto V$; E/s falls

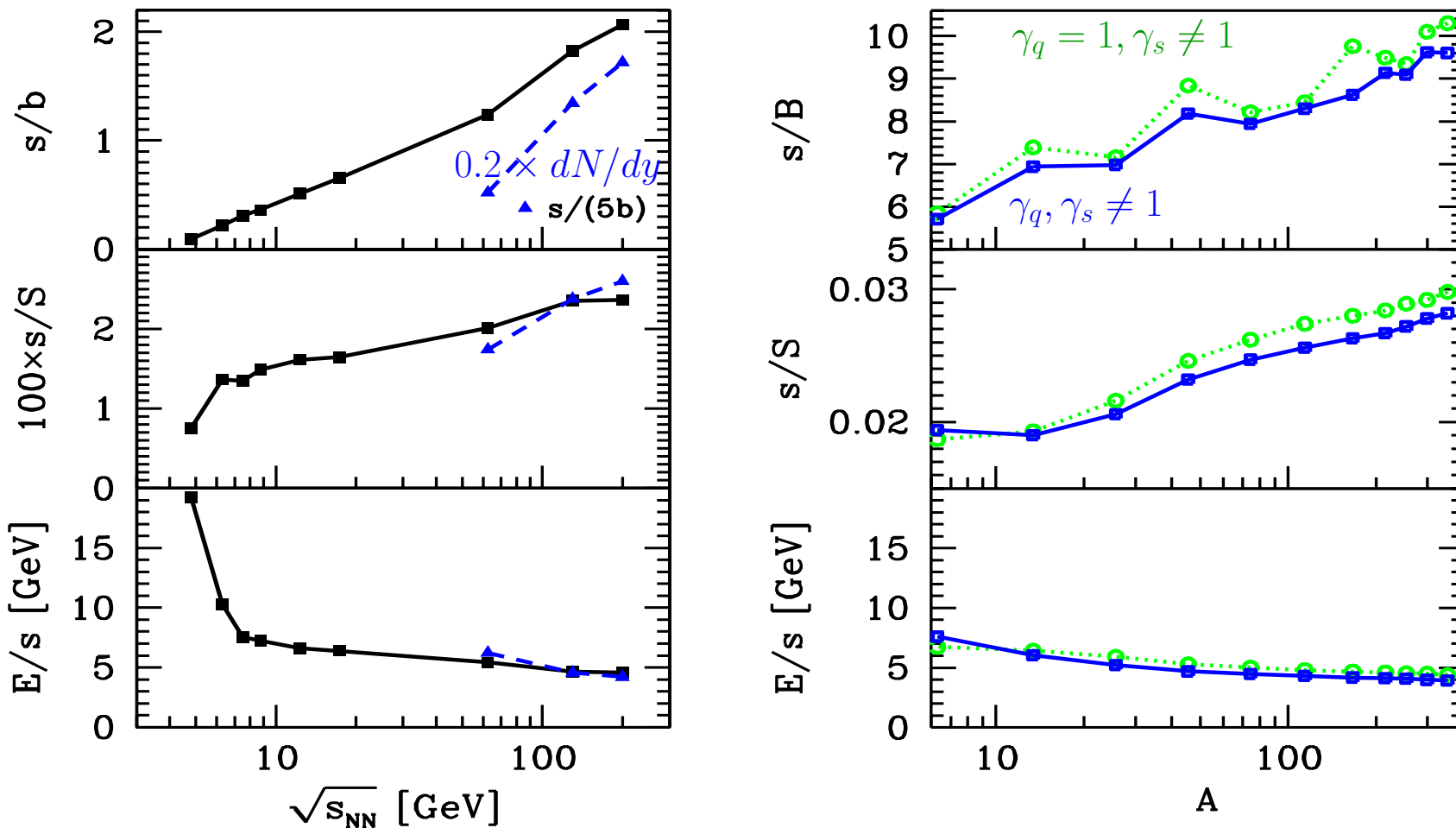


Showing results for both $\gamma_q, \gamma_s \neq 1$, for $\gamma_s \neq 1, \gamma_q = 1$. Note little difference in the result, even though the value of T will differ significantly.

- 1) $s/S \rightarrow 0.027$, as function of V ;
- 2) most central value near QGP chemical equilibrium;
- 3) no saturation for largest volumes available;

Behavior is consistent with QGP prediction of steady increase of strangeness yield with increase of the volume, which implies longer lifespan and hence greater strangeness yield, both specific yield and larger γ_s^{QGP} .

COMPARE $\sqrt{s_{NN}}$ and V dependence of s/b and s/S , E/s



Full 4π and central rapidity results.

We again find $s/S \rightarrow 0.027$, as function of $\sqrt{s_{NN}}$ and V : no saturation, consistent with QGP expectation and $\gamma_s^{\text{QGP}} \simeq 1$, confirmed by s/B .

Energy/strangeness E/s cost drop at $\sqrt{s_{NN}^{\text{CR}}}$, suggests appearance of a new (e.g. $GG \rightarrow s\bar{s}$) production mechanism.

Strangeness / Entropy in QGP

Relative s/S yield measures the number of active degrees of freedom and the degree of relaxation when strangeness production freezes-out. **Perturbative expression in chemical equilibrium:**

$$\frac{s}{S} = \frac{\frac{g_s}{2\pi^2} T^3 (m_s/T)^2 K_2(m_s/T)}{(g_2 \pi^2/45) T^3 + (g_s n_f/6) \mu_q^2 T} \simeq \frac{1}{35} = 0.0286$$

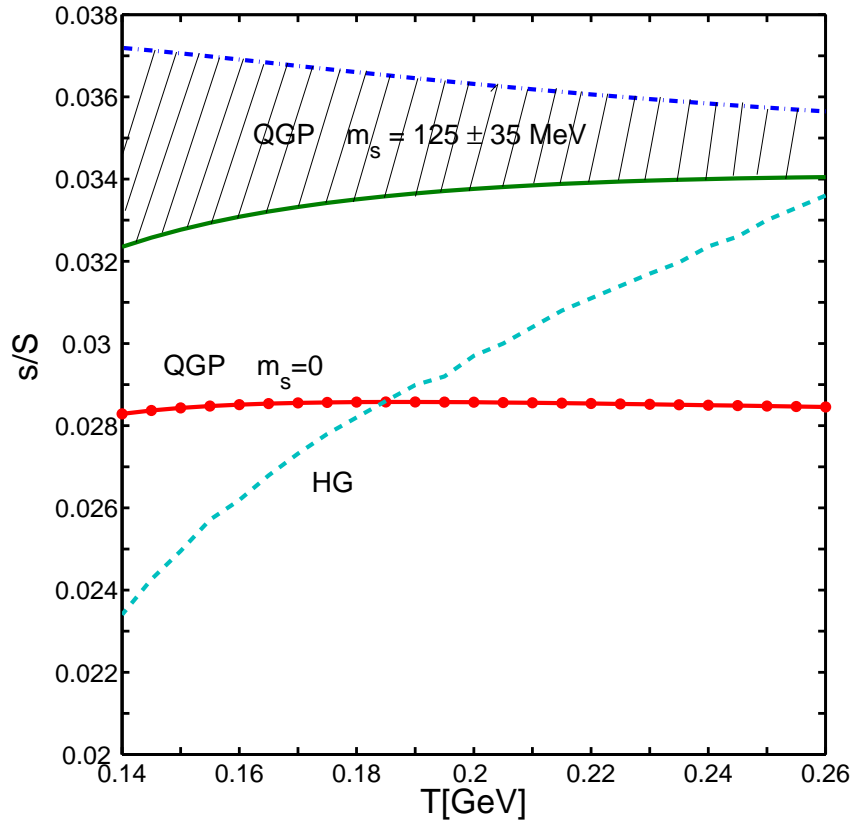
much of $\mathcal{O}(\alpha_s)$ interaction effect cancels out. When considered $s/S \rightarrow 1/31 = 0.0323$

Allow for chemical non-equilibrium of strangeness γ_s^{QGP} , and possible quark-gluon pre-equilibrium – gradual increase to the limit expected:

$$\frac{s}{S} = \frac{0.03 \gamma_s^{\text{QGP}}}{0.4 \gamma_G + 0.1 \gamma_s^{\text{QGP}} + 0.5 \gamma_q^{\text{QGP}} + 0.05 \gamma_q^{\text{QGP}} (\ln \lambda_q)^2} \rightarrow 0.03.$$

We expect the yield of gluons and light quarks to approach chemical equilibrium fast and first: $\gamma_G \rightarrow 1$ and $\gamma_q^{\text{QGP}} \rightarrow 1$, thus $s/S \simeq 0.03 \gamma_s^{\text{QGP}}$.

CHECK: FIT YIELDS OF PARTICLES, EVALUATE STRANGENESS AND ENTROPY CONTENT AND COMPARE WITH EXPECTED RATIO, THEORETICAL STUDY HOW BIG s/S can be at LHC, help for phase transition at low μ_B



Strangeness to entropy ratio s/S as function of temperature T , for the QGP (green, solid line for $m_s = 160 \text{ MeV}$, blue dash-dot line for $m_s = 90 \text{ MeV}$) with $k = 1$; and for HG (light blue, dashed line) phases for $\gamma_q = \gamma_s = \lambda_q = \lambda_s = 1$ in both phases. The line with points (red) corresponds to s/S obtained for $m_s = 0$.

Value of $s/S \simeq 1/30$ is ratio of strange to all degrees of freedom s/S greater in QGP compared to HG at same T = enhancement of strangeness at hadronization. The lowering of s yield for $m_s \rightarrow 0$ due to growth of perturbative QCD interaction.

END LECTURE ONE

LECTURE TWO

Statistical Hadronization fits of hadron yields

Full analysis of experimental hadron yield results requires a significant numerical effort in order to allow for resonances, particle widths, full decay trees, isospin multiplet sub-states.

Kraków-Tucson (and SHARE 2 Montreal) collaboration produced a public package **SHARE Statistical Hadronization with Resonances** which is available e.g. at

<http://www.physics.arizona.edu/~torrieri/SHARE/share.html>

Lead author: **Giorgio Torrieri**

GT, W. Broniowski, W. Florkowski, J. Letessier, S. Steinke, JR
nucl-th/0404083 Comp. Phys. Com. 167, 229 (2005)

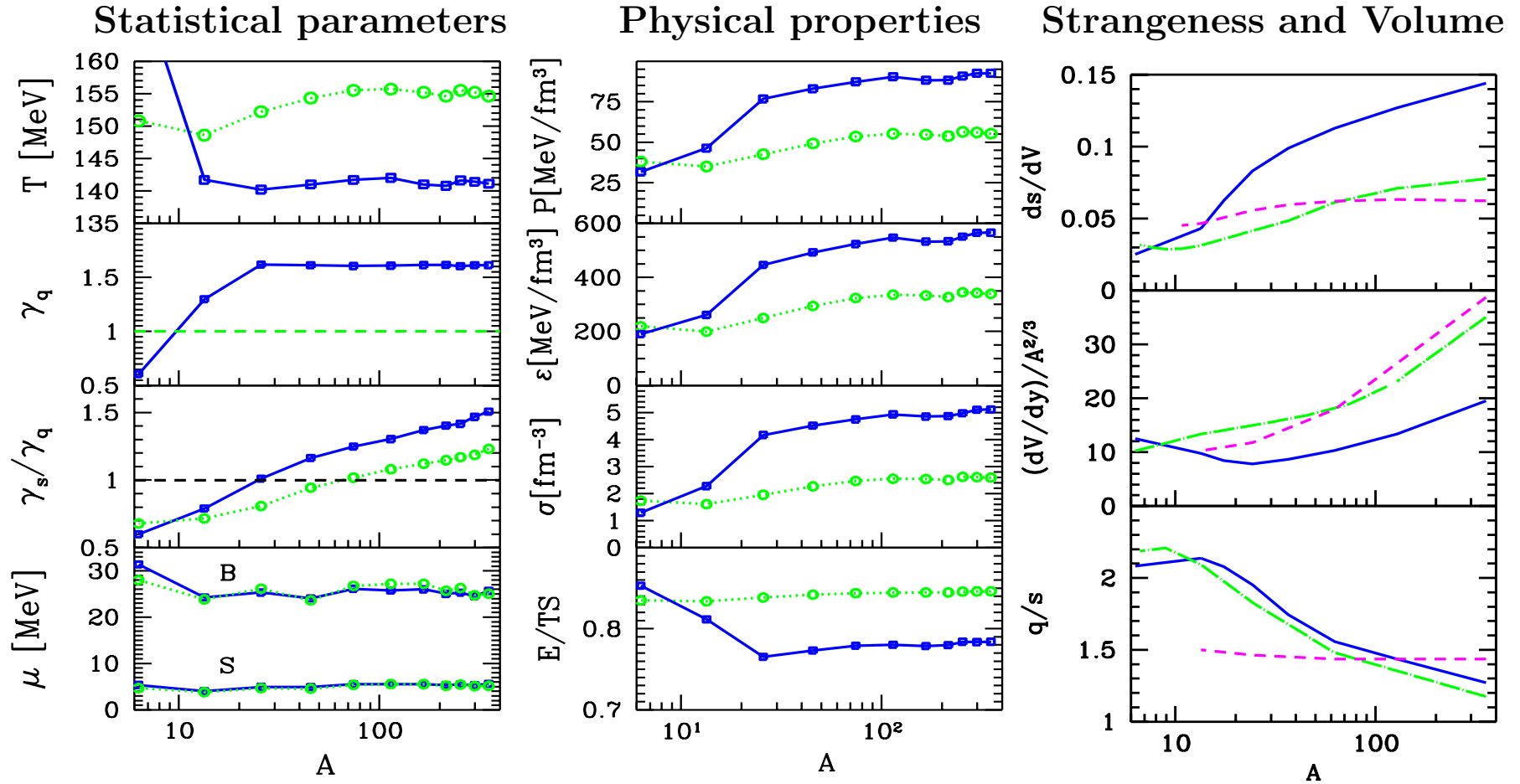
SHARE 2 with flexible weak decays, fluctuations and chemical flexibility now on line and in review. Involves S.Y. Jeon, Montreal (of fluctuation fame)

Aside of particle yields, also PHYSICAL PROPERTIES of the source are available, both in SHARE and ONLINE.

DATA: Centrality dependence of dN/dy for π^\pm , K^\pm , p and \bar{p} . The errors are systematic only. The statistical errors are negligible. PHENIX data

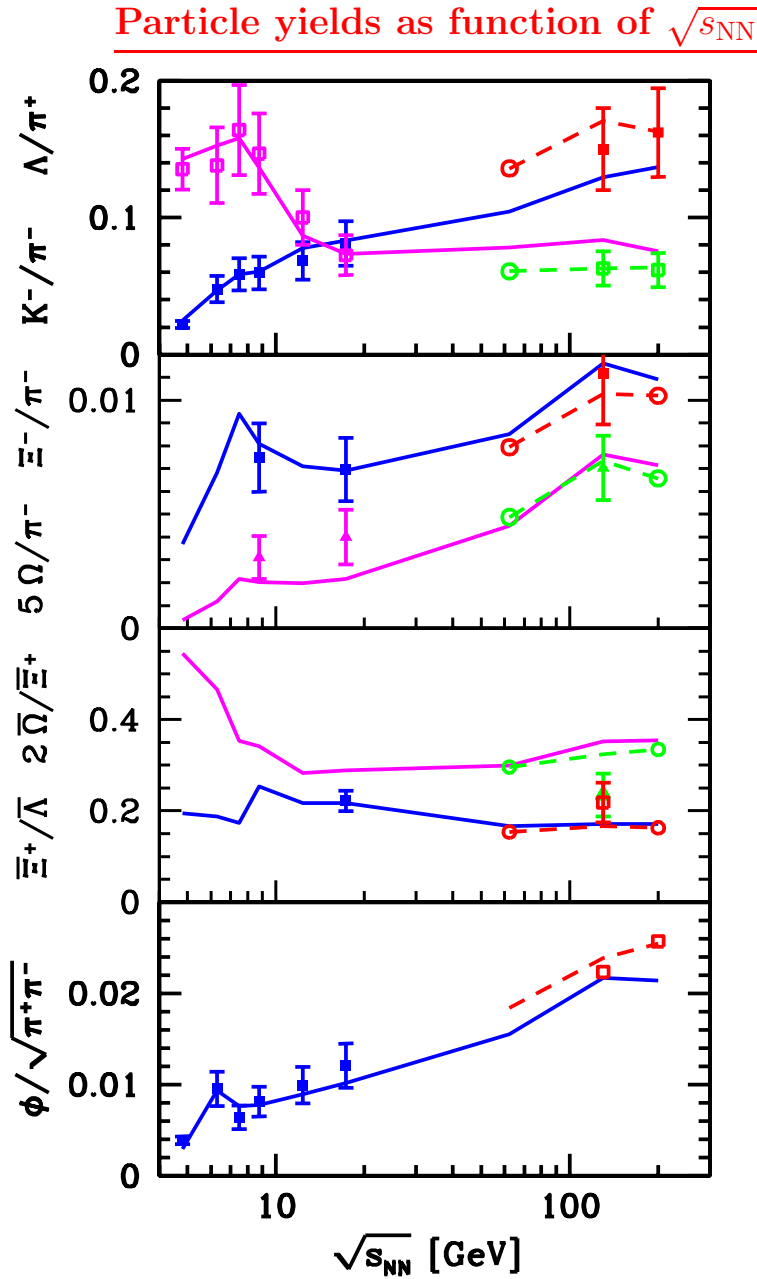
N_{part}	π^+	π^-	K^+	K^-	p	\bar{p}
351.4	286.4 ± 24.2	281.8 ± 22.8	48.9 ± 6.3	45.7 ± 5.2	18.4 ± 2.6	13.5 ± 1.8
299.0	239.6 ± 20.5	238.9 ± 19.8	40.1 ± 5.1	37.8 ± 4.3	15.3 ± 2.1	11.4 ± 1.5
253.9	204.6 ± 18.0	198.2 ± 16.7	33.7 ± 4.3	31.1 ± 3.5	12.8 ± 1.8	9.5 ± 1.3
215.3	173.8 ± 15.6	167.4 ± 14.4	27.9 ± 3.6	25.8 ± 2.9	10.6 ± 1.5	7.9 ± 1.1
166.6	130.3 ± 12.4	127.3 ± 11.6	20.6 ± 2.6	19.1 ± 2.2	8.1 ± 1.1	5.9 ± 0.8
114.2	87.0 ± 8.6	84.4 ± 8.0	13.2 ± 1.7	12.3 ± 1.4	5.3 ± 0.7	3.9 ± 0.5
74.4	54.9 ± 5.6	52.9 ± 5.2	8.0 ± 0.8	7.4 ± 0.6	3.2 ± 0.5	2.4 ± 0.3
45.5	32.4 ± 3.4	31.3 ± 3.1	4.5 ± 0.4	4.1 ± 0.4	1.8 ± 0.3	1.4 ± 0.2
25.7	17.0 ± 1.8	16.3 ± 1.6	2.2 ± 0.2	2.0 ± 0.1	0.93 ± 0.15	0.71 ± 0.12
13.4	7.9 ± 0.8	7.7 ± 0.7	0.89 ± 0.09	0.88 ± 0.09	0.40 ± 0.07	0.29 ± 0.05
6.3	4.0 ± 0.4	3.9 ± 0.3	0.44 ± 0.04	0.42 ± 0.04	0.21 ± 0.04	0.15 ± 0.02

and STAR ϕ and K^* yields



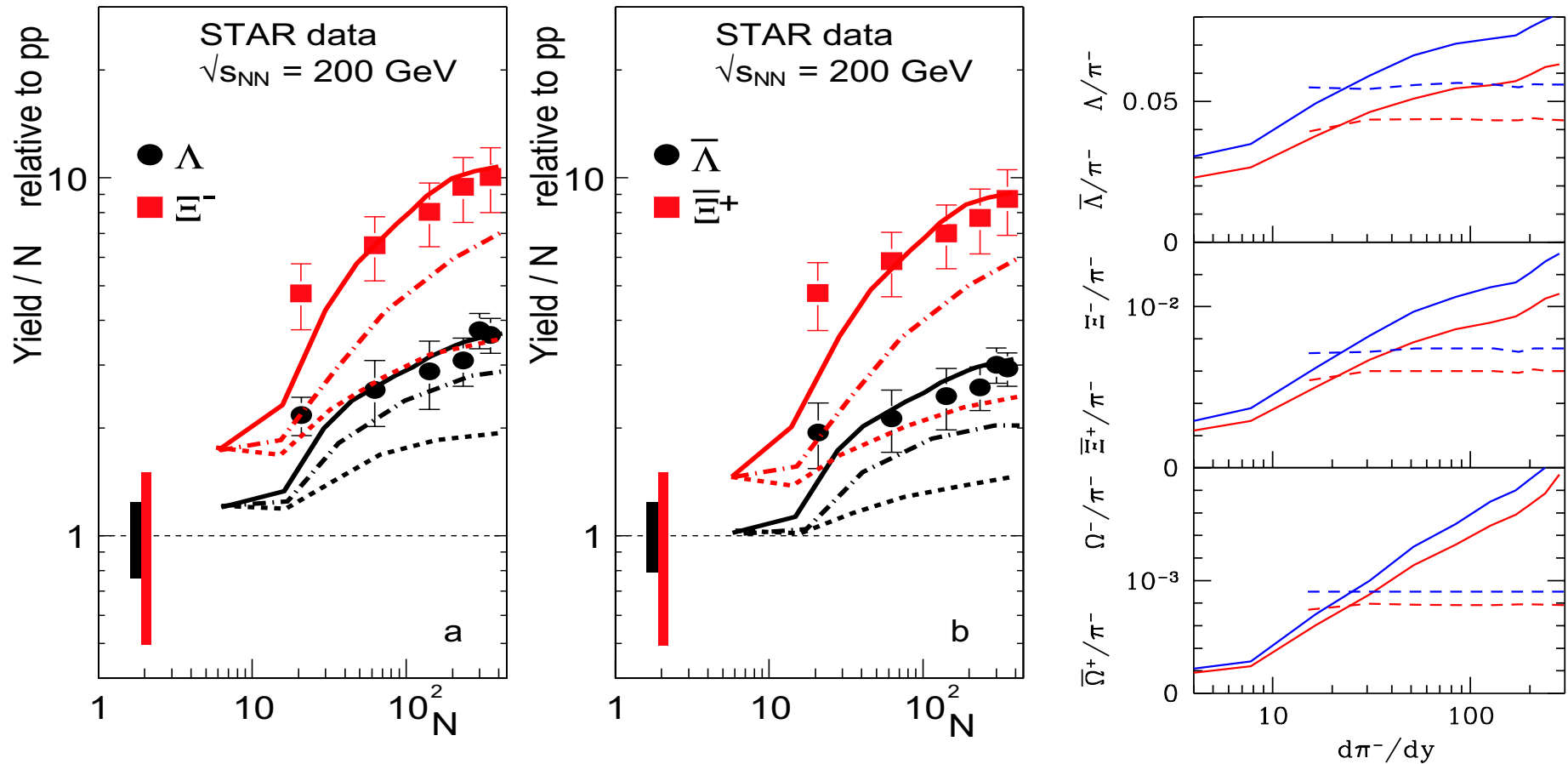
LINES: $\gamma_s, \gamma_q \neq 1$ and $\gamma_s \neq 1, \gamma_q = 1$, also $\gamma_s = \gamma_q = 1$
 γ_q changes with $A \propto V$ from under-saturated to over-saturated value, γ_s^{HG} increases steadily to 2.4, implying near saturation in QGP. P, σ, ϵ increase by factor 2–3, at $A > 20$ (onset of new physics?), E/TS decreases with A .

Statistical + fit errors are seen in fluctuations, systematic error impacts absolute normalization by $\pm 10\%$.



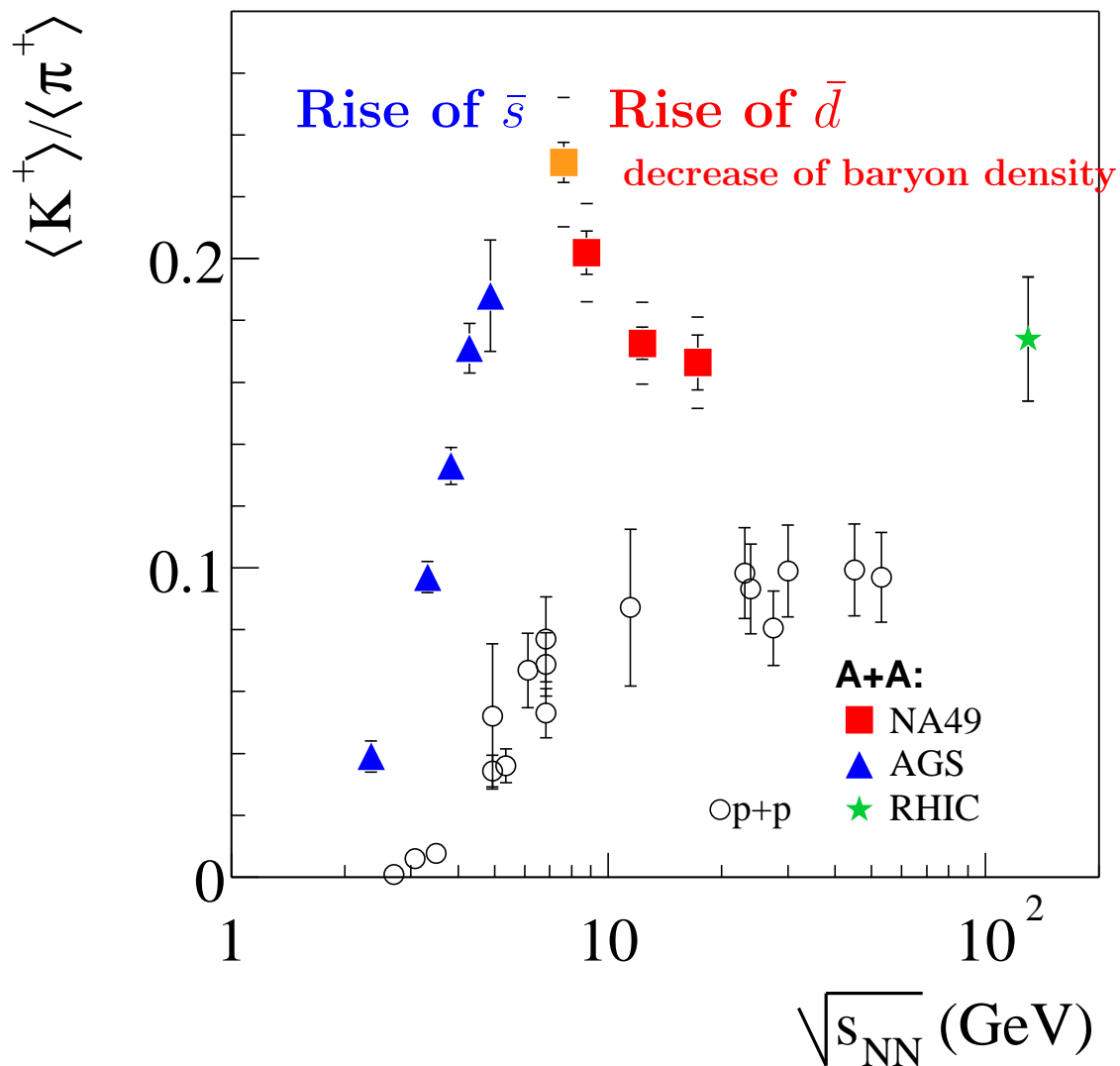
$\sqrt{s_{NN}}$ [GeV]	$N_{4\pi}$ 5%			$dN/dy _{y=0}$ 5%		
	62.4	130	200	62.4	130	200
b	350.2	350.2	350.1	32.64	19.79	14.8
π^+	1001	1282	1470	225.8	236.6	237.4
π^-	1072	1368	1558	236.7	246.8	247.2
K^+	194.5	289.9	297.9	43.3	49.5	50.7
K^-	139.4	222.5	236.3	37.5	45.5	47.6
K_S	162.3	248.2	259.2	39.2	45.9	47.5
ϕ	18.6	34.6	32.9	4.96	6.58	7.06
p	156.5	163.9	177.5	21.56	18.91	18.02
\bar{p}	25.9	40.7	50.6	9.77	12.05	12.95
Λ	68.6	89.3	89.0	12.3	11.4	11.4
$\bar{\Lambda}$	16.0	29.1	32.2	5.91	7.94	8.7
Ξ^-	11.3	18.1	16.5	2.18	2.60	2.70
Ξ^+	3.7	7.85	7.67	1.34	1.97	2.21
Ω	1.13	2.37	1.97	0.27	0.38	0.42
$\bar{\Omega}$	0.56	1.40	1.21	0.20	0.32	0.37
$K^0(892)$	47.9	70.1	80.0	19.5	11.8	12.1
Δ^0	28.8	28.5	31.3	3.76	3.22	3.05
Δ^{++}	27.2	27.8	30.6	3.71	3.19	3.03
$\Lambda(1520)$	4.43	5.73	5.76	0.72	0.73	0.73
$\Sigma^+(1385)$	8.50	10.94	10.93	1.37	1.38	1.37
$\Xi^0(1530)$	2.98	4.90	4.45	0.59	0.71	0.74
η	110.2	158.7	172.7	26.3	29.6	30.3
η'	8.45	13.03	13.75	2.08	2.44	2.54
ρ^0	84.4	106	125	18.9	19.5	19.6
$\omega(782)$	75.5	94.9	112.2	17.1	17.6	17.6
$f_0(980)$	7.08	10.79	11.47	1.74	2.02	2.09

RHIC200 PREDICTION OF dependence on centrality



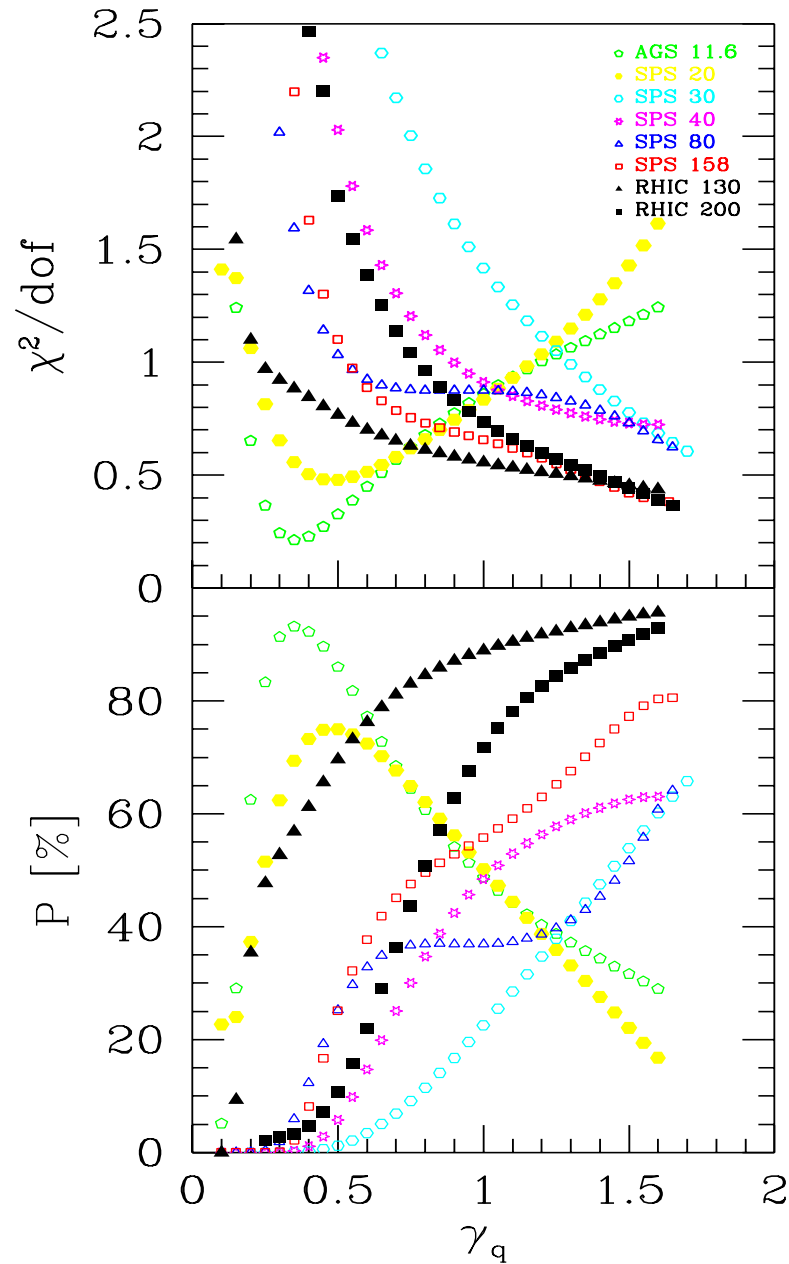
STAR $\sqrt{s_{NN}} = 200$ GeV yields of hyperons $d\Lambda/dy$ and $d\Xi^-/dy$, (a), and antihyperons $d\bar{\Lambda}/dy$ and $d\bar{\Xi}^+/dy$, (b), normalized with, and as function of, A , relative to these yields in pp reactions: $d(\Lambda + \bar{\Lambda})/dy = 0.066 \pm 0.006$, $d(\Xi^- + \bar{\Xi}^+)/dy = 0.0036 \pm 0.0012$, $\bar{\Lambda}/\Lambda = 0.88 \pm 0.09$ and $\bar{\Xi}^+/\Xi^- = 0.90 \pm 0.09$. **Solid lines, chemical non-equilibrium, dashed chemical equilibrium, (dash-dotted lines, semi-equilibrium.)** On right, the predicted hyperons per π^- yields (blue for hyperons and for antihyperons).

MOST SPECTACULAR

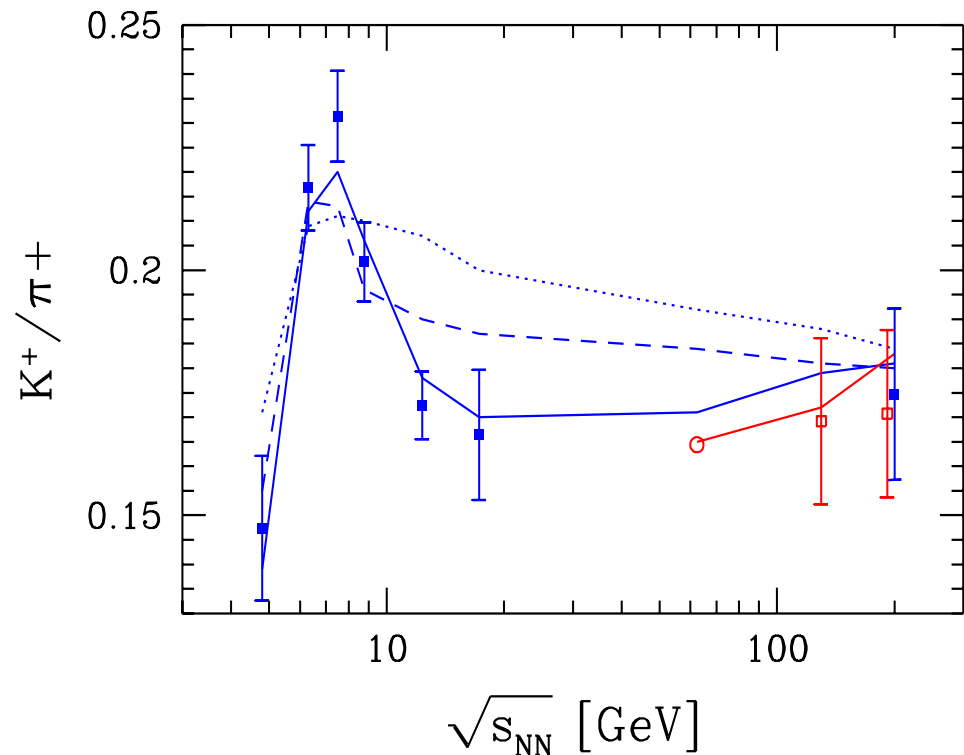


The NA49 (Marek Gaździcki) HORN

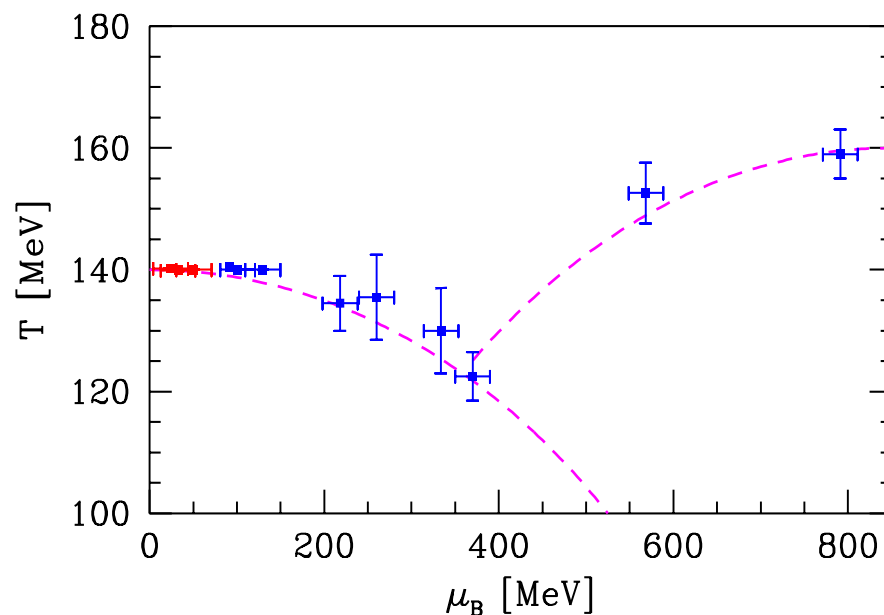
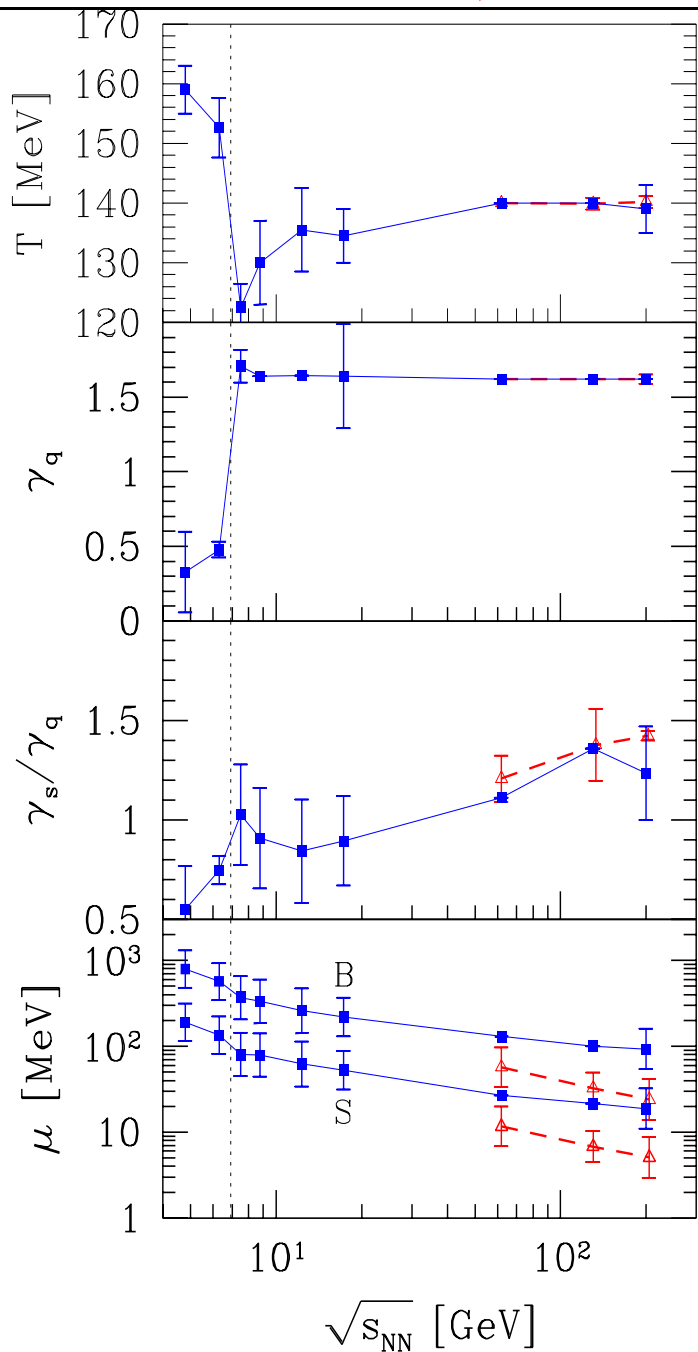
To describe the horn we need $\gamma_q \neq 1$



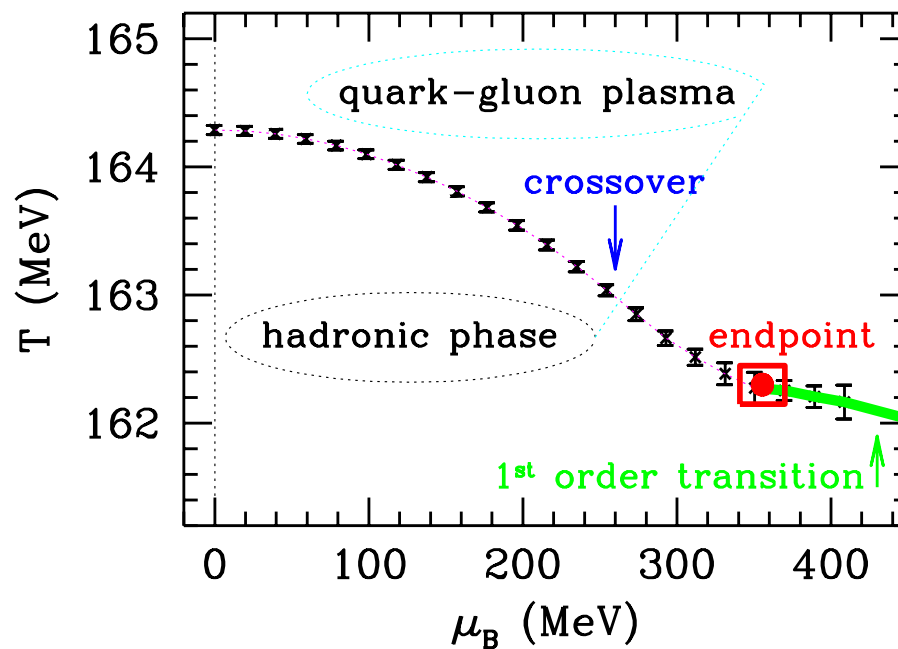
Looking at the fit χ^2 we see that between 20 and 30 GeV results favor that γ_q jumps from highly unsaturated to fully saturated: **from $\gamma_q < 0.5$ to $\gamma_q > 1.5$. This produces the horn (below). The individual fits relevant to understanding how the horn is created have good quality - see $P\%$.**



SUMMARY OF $\sqrt{s_{NN}}$ FIT RESULTS: Statistical parameters



to be compared to, see below:

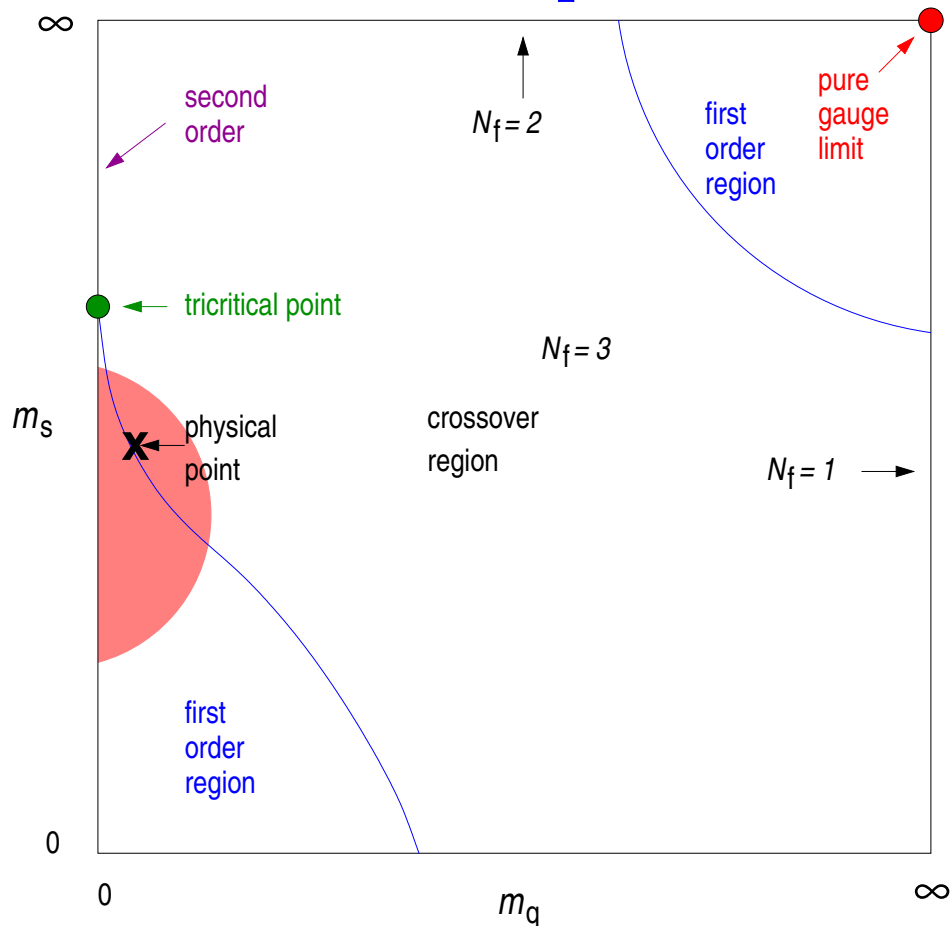


Why low/high PHASE BOUNDARY Temperature?

- Dynamical effects of expansion:
colored partons like a wind, displace the boundary
- Degrees of freedom
 - Temperature of phase transition depends on available degrees of freedom.
For 2+1 flavors: $T = 162 \pm 3$, for $\gamma_s \rightarrow 0$
 $2 + 1 \rightarrow 2$ flavor theory with $T \rightarrow 170$ MeV,
what happens when $\gamma_s \rightarrow 1.5$?
 - The nature of phase transition/transformation changes when number of flavors rises from 2+1 to 3 is effect of $\gamma_i > 1$ creating a real phase transition?
- at high μ_B we encounter
 - either conventional hadrons (contradiction with continuity of quark related variables: strangeness, strange antibaryons).
 - or more likely, a new heavy (valon) quark phases.
Under saturation of phase space compatible with higher T .

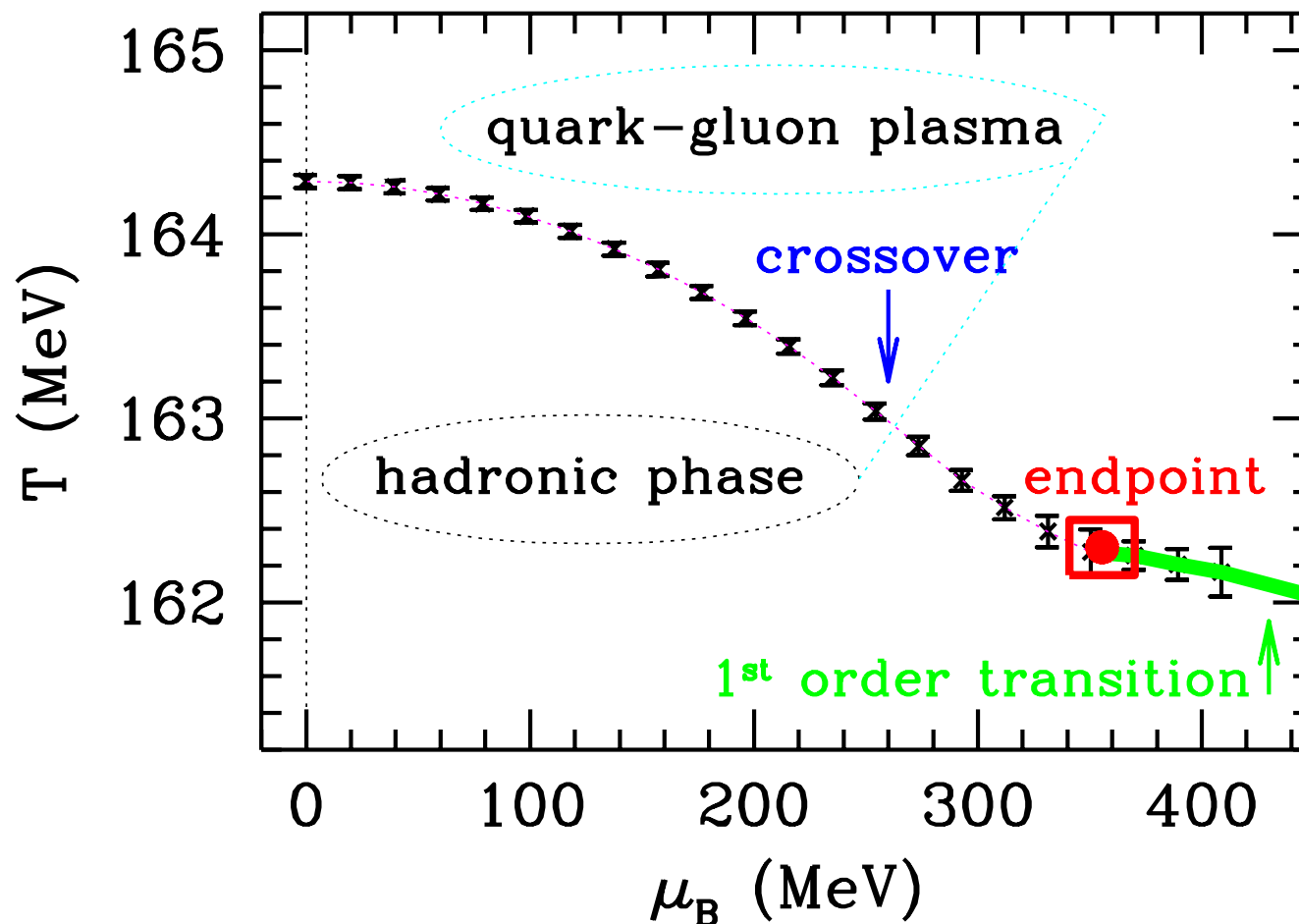
Evidence for these arguments in the physical properties:

Fermi degrees of freedom and phase transitions in QCD



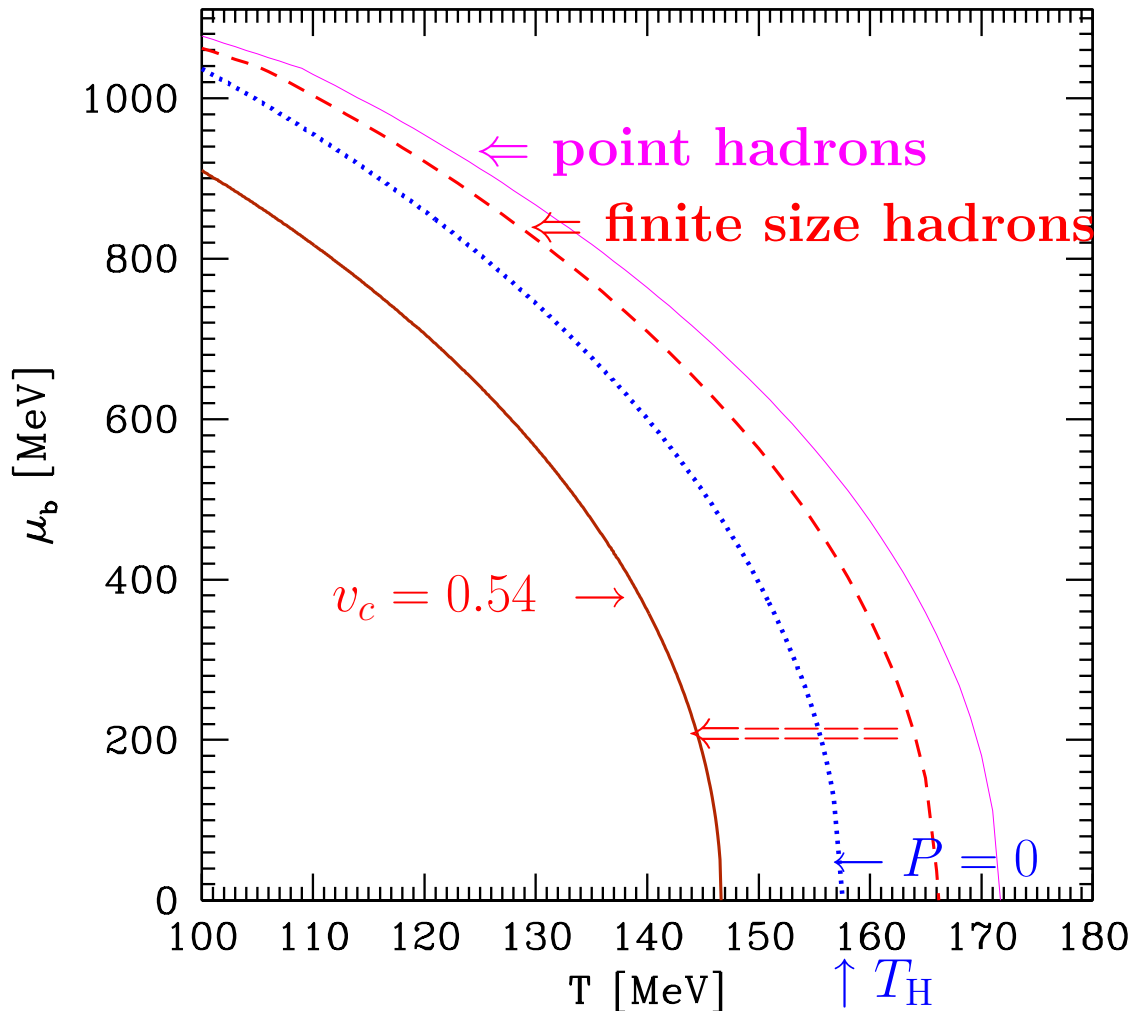
adapted from: THE THREE FLAVOR CHIRAL PHASE TRANSITION WITH AN IMPROVED QUARK AND GLUON ACTION IN LATTICE QCD. By A. Peikert, F. Karsch, E. Laermann, B. Sturm, (LATTICE 98), Boulder, CO, 13-18 Jul 1998. in Nucl.Phys.Proc.Suppl.73:468-470,1999. Note that we need some additional quark degrees of freedom to push the system over to phase transition. Conventional wisdom: baryon density:

...and considering the baryochemical potential



adapted from: CRITICAL POINT OF QCD AT FINITE T AND μ , LATTICE RESULTS FOR PHYSICAL QUARK MASSES. By Z. Fodor, S.D. Katz (Wuppertal U.), JHEP 0404:050,2004; hep-lat/0402006. However, at LHC the baryochemical potential at level of 1-3 MeV. Better hope for γ_s , and **MOTION**:

(dynamical) Phase boundary and ‘wind’ of flow of matter



Solid: point hadrons T_p
Dashed: finite size hadrons
Thick solid: breakup with $v = 0.54$ ($\kappa = 0.6$)
Expansion
SUPERCOOLING
by 20 MeV

$T_H = 158$ MeV Hagedorn temperature where $P = 0$, no hadron P
 $T_f \simeq 0.9T_H \simeq 143$ MeV is where supercooled QGP fireball breaks up
 equilibrium phase transformation used here was at $T \simeq 166$.

SUDDEN MECHANISM: Super-cooling COLOR WIND of an exploding fireball

P and ε : local in QGP particle pressure, energy density, \vec{v} local flow velocity.
The pressure component in the energy-momentum tensor:

$$T^{ij} = P\delta_{ij} + (P + \varepsilon)\frac{v_i v_j}{1 - \vec{v}^2}.$$

The rate of momentum flow vector $\vec{\mathcal{P}}$ at the surface of the fireball is obtained from the energy-stress tensor T_{kl} :

$$\vec{\mathcal{P}} \equiv \hat{T} \cdot \vec{n} = P\vec{n} + (P + \varepsilon)\frac{\vec{v}_c \vec{v}_c \cdot \vec{n}}{1 - \vec{v}_c^2}.$$

The pressure and energy comprise particle and the vacuum properties: $P = P_p - \mathcal{B}$, $\varepsilon = \varepsilon_p + \mathcal{B}$. Condition $\vec{\mathcal{P}} = 0$ reads:

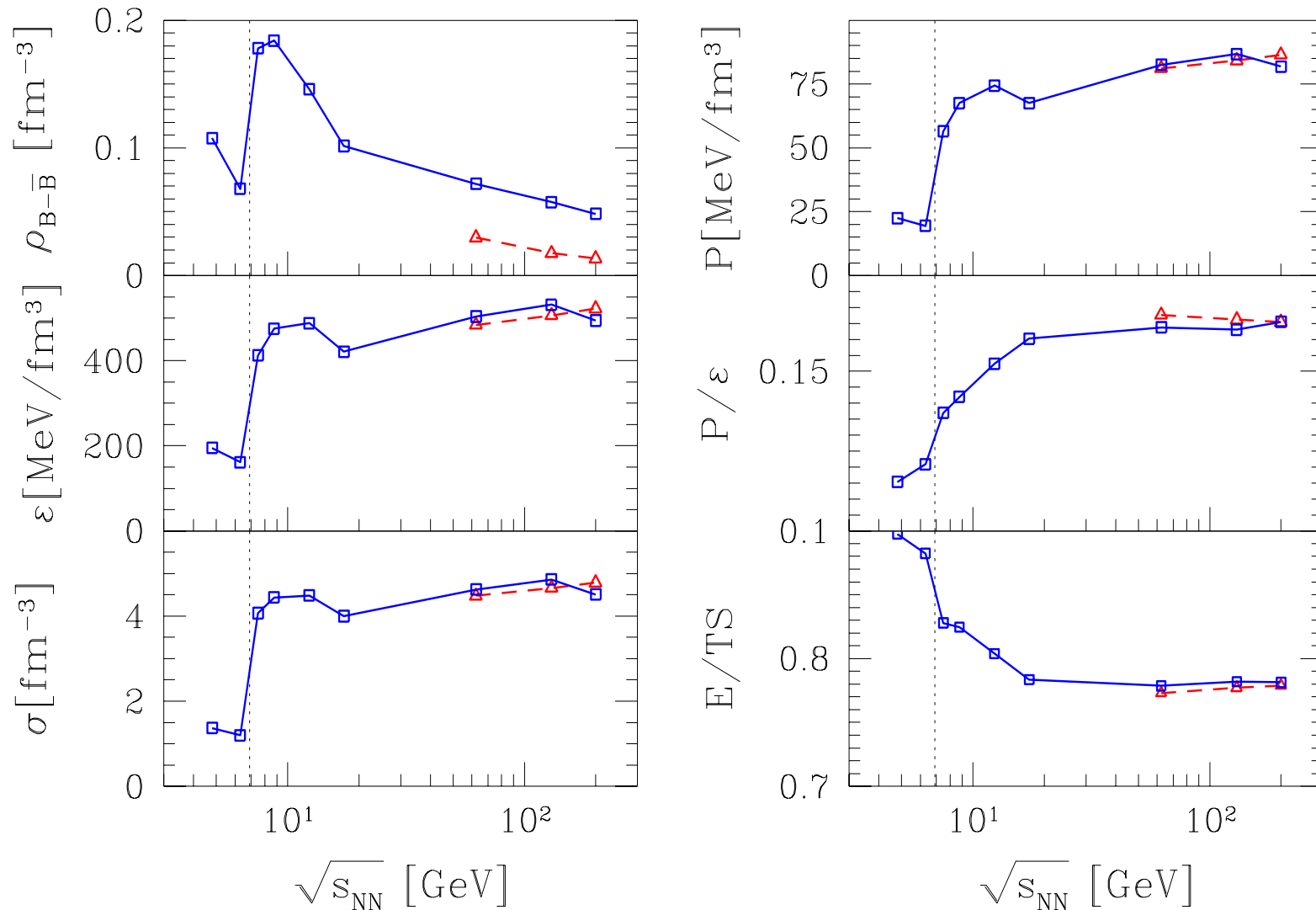
$$\mathcal{B}\vec{n} = P_p\vec{n} + (P_p + \varepsilon_p)\frac{\vec{v}_c \vec{v}_c \cdot \vec{n}}{1 - v_c^2},$$

Multiplying with \vec{n} , we find,

$$\mathcal{B} = P_p + (P_p + \varepsilon_p)\frac{\kappa v_c^2}{1 - v_c^2}, \quad \kappa = \frac{(\vec{v}_c \cdot \vec{n})^2}{v_c^2}.$$

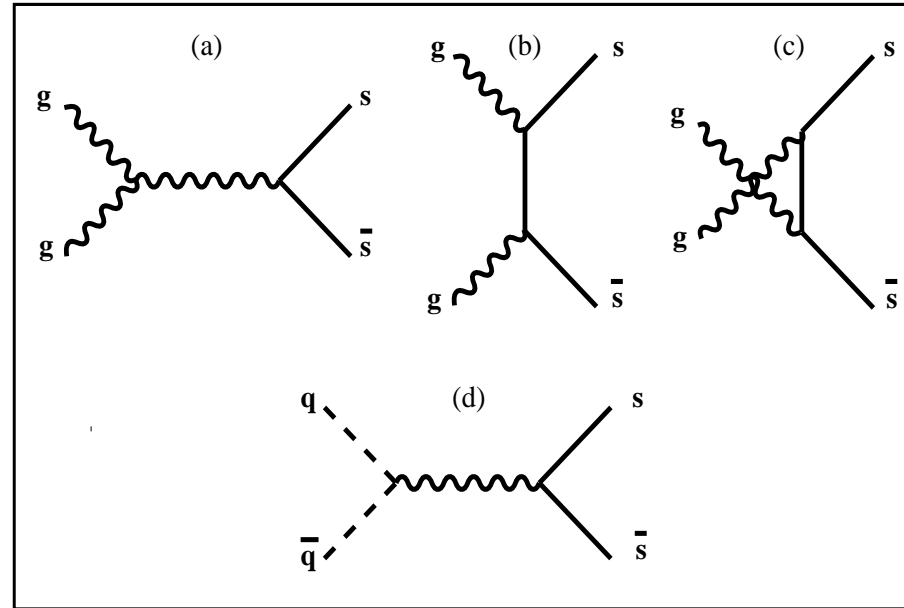
This requires $P_p < \mathcal{B}$: QGP phase pressure P must be NEGATIVE. A fireball surface region which reaches $\mathcal{P} \rightarrow 0$ and continues to flow outward is torn apart in a rapid instability. This can ONLY arise since matter presses against the vacuum which is not subject to collective dynamics.

PHYSICAL PROPERTIES as function of $\sqrt{s_{NN}}$



Note that behavior is the same as we saw as function of A : the large jumps by factor 2–3 in densities (to left) and pressure (on right) as the collision energy changes from 20 GeV to 30 GeV. **There is clear evidence of change in reaction mechanism.** There no difference between top SPS and RHIC energy range.

Kinetic strangeness production



The generic angle averaged cross sections for (heavy) flavor s , \bar{s} production processes $g + g \rightarrow s + \bar{s}$ and $q + \bar{q} \rightarrow s + \bar{s}$, are:

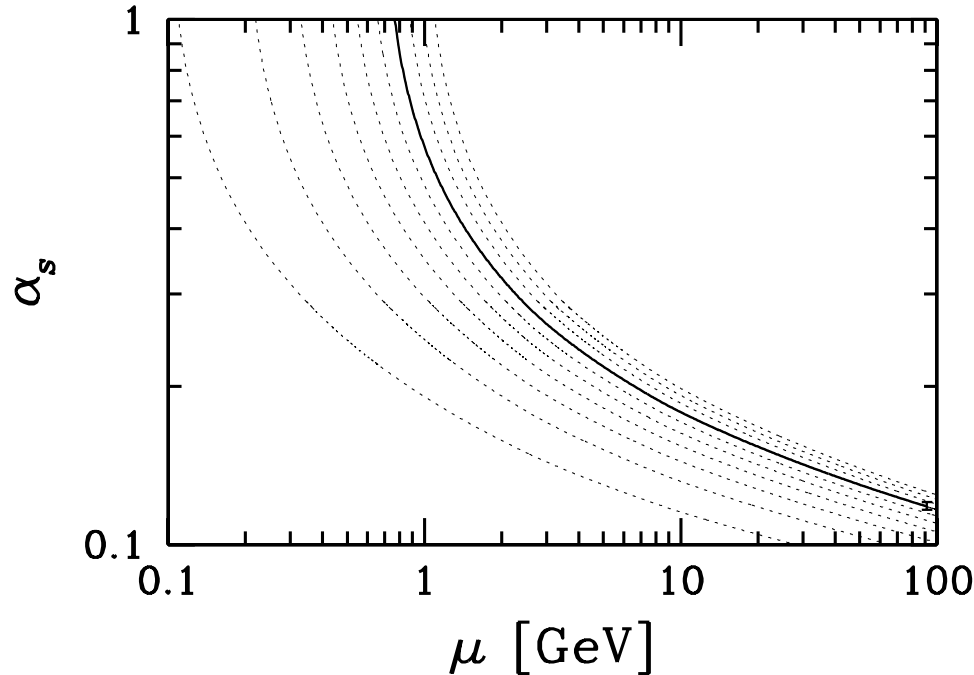
$$\bar{\sigma}_{gg \rightarrow s\bar{s}}(s) = \frac{2\pi\alpha_s^2}{3s} \left[\left(1 + \frac{4m_s^2}{s} + \frac{m_s^4}{s^2} \right) \tanh^{-1}W(s) - \left(\frac{7}{8} + \frac{31m_s^2}{8s} \right) W(s) \right],$$

$$\bar{\sigma}_{q\bar{q} \rightarrow s\bar{s}}(s) = \frac{8\pi\alpha_s^2}{27s} \left(1 + \frac{2m_s^2}{s} \right) W(s). \quad W(s) = \sqrt{1 - 4m_s^2/s}$$

Infinite QCD resummation: running α_s and m_s taken at the energy scale $\mu \equiv \sqrt{s}$.
USED: $m_s(M_Z) = 90 \pm 20\%$ MeV $m_s(1\text{GeV}) \simeq 2.1m_s(M_Z) \simeq 200\text{MeV}$.

WHY PERTURBATIVE STRANGENESS WORKS

An essential pre-requirement for the perturbative theory of strangeness production in QGP, is the relatively small experimental value $\alpha_s(M_Z) \simeq 0.118$, which has been experimentally established in recent years.



$\alpha_s^{(4)}(\mu)$ as function of energy scale μ for a variety of initial conditions. Solid line: $\alpha_s(M_Z) = 0.1182$ (experimental point, includes the error bar at $\mu = M_Z$).

At the scale of just above 1 GeV where typically thermal strangeness production in RHIC QGP occurs, perturbative theory makes good sense but is not completely reliable. **Had $\alpha_s(M_Z) > 0.125$ been measured 1996 than our perturbative strangeness production approach from 1982 would have been invalid.**

Thermal average of (strangeness production) reaction rates

Kinetic (momentum) equilibration is faster than chemical, use thermal particle distributions $f(\vec{p}_1, T)$ to obtain average rate:

$$\langle \sigma v_{\text{rel}} \rangle_T \equiv \frac{\int d^3 p_1 \int d^3 p_2 \sigma_{12} v_{12} f(\vec{p}_1, T) f(\vec{p}_2, T)}{\int d^3 p_1 \int d^3 p_2 f(\vec{p}_1, T) f(\vec{p}_2, T)}.$$

Invariant reaction rate in medium:

$$A^{gg \rightarrow s\bar{s}} = \frac{1}{2} \rho_g^2(t) \langle \sigma v \rangle_T^{gg \rightarrow s\bar{s}}, \quad A^{q\bar{q} \rightarrow s\bar{s}} = \rho_q(t) \rho_{\bar{q}}(t) \langle \sigma v \rangle_T^{q\bar{q} \rightarrow s\bar{s}}, \quad A^{s\bar{s} \rightarrow gg, q\bar{q}} = \rho_s(t) \rho_{\bar{s}}(t) \langle \sigma v \rangle_T^{s\bar{s} \rightarrow gg, q\bar{q}}.$$

$1/(1 + \delta_{1,2})$ introduced for two gluon processes compensates the double-counting of identical particle pairs, arising since we are summing independently both reacting particles.

This rate enters the momentum-integrated Boltzmann equation which can be written in form of current conservation with a source term

$$\partial_\mu j_s^\mu \equiv \frac{\partial \rho_s}{\partial t} + \frac{\partial \vec{v} \rho_s}{\partial \vec{x}} = A^{gg \rightarrow s\bar{s}} + A^{q\bar{q} \rightarrow s\bar{s}} - A^{s\bar{s} \rightarrow gg, q\bar{q}}$$

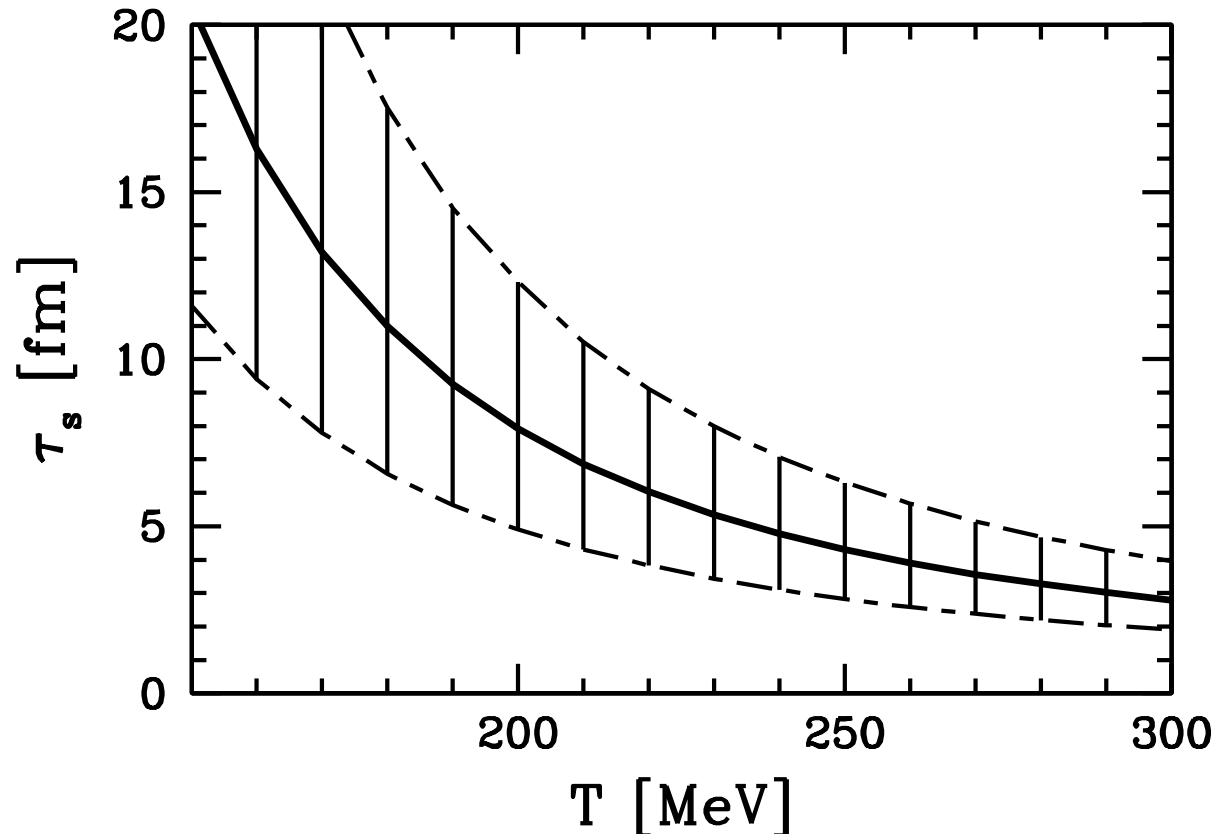
Strangeness relaxation to chemical equilibrium

Strangeness density time evolution in local rest frame:

$$\frac{d\rho_s}{d\tau} = \frac{d\rho_{\bar{s}}}{d\tau} = \frac{1}{2}\rho_g^2(t) \langle \sigma v \rangle_T^{gg \rightarrow s\bar{s}} + \rho_q(t)\rho_{\bar{q}}(t) \langle \sigma v \rangle_T^{q\bar{q} \rightarrow s\bar{s}} - \rho_s(t)\rho_{\bar{s}}(t) \langle \sigma v \rangle_T^{s\bar{s} \rightarrow gg, q\bar{q}}$$

Evolution for s and \bar{s} identical, which allows to set $\rho_s(t) = \rho_{\bar{s}}(t)$.
characteristic time constant τ_s :

$$2\tau_s \equiv \frac{\rho_s(\infty)}{A_{gg \rightarrow s\bar{s}} + A_{q\bar{q} \rightarrow s\bar{s}} + \dots} \quad A^{12 \rightarrow 34} \equiv \frac{1}{1+\delta_{1,2}} \gamma_1 \gamma_2 \rho_1^\infty \rho_2^\infty \langle \sigma_s v_{12} \rangle_T^{12 \rightarrow 34} .$$



STRANGENESS IN ENTROPY CONSERVING EXPANSION

QGP expansion is adiabatic i.e. ($g_G = 2_s 8_c = 16, g_q = 2_s 3_c n_f$)

$$S = \frac{4\pi^2}{90} g(T) V T^3 = \mathbf{Const.} \quad g = g_G \left(1 - \frac{15\alpha_s(T)}{4\pi} + \dots \right) + \frac{7}{4} g_q \left(1 - \frac{50\alpha_s(T)}{21\pi} + \dots \right) .$$

The volume, temperature change such that $\delta(gT^3V) = 0$. Strangeness phase space occupancy, $g_s = 2_s 3_c \left(1 - \frac{k\alpha_s(T)}{\pi} + \dots \right)$, $k = 2$ for $m_s/T \rightarrow 0$:

$$\gamma_s(\tau) \equiv \frac{n_s(\tau)}{n_s^\infty(T(\tau))}, \quad n_s(\tau) = \gamma_s(\tau) T(\tau)^3 \frac{g_s(T)}{2\pi^2} z^2 K_2(z), \quad z = \frac{m_s}{T(t)}, \quad K_i : \text{Bessel f.}$$

evolves due to production and **dilution**, keeping entropy fixed:

$$\frac{d\gamma_s}{d\tau} + \gamma_s \frac{d \ln[g_s z^2 K_2(z)/g]}{d\tau} = \frac{A_G}{2n_s^\infty} [\gamma_G^2 - \gamma_s^2] + \frac{A_q}{2n_s^\infty} [\gamma_q^2 - \gamma_s^2]$$

For $m_s \rightarrow 0$ **dilution effect decreases, disappears, and $\gamma_s \leq \gamma_{G,q}$, importance grows with mass of the quark, $z = m_s(T)/T$, which grows near phase transition boundary. From this we can obtain the time evolution of s/S , the specific strangeness per entropy:**

$$\frac{d}{d\tau} \frac{s}{S} = \frac{g_s}{g} z^2 K_2(z) \left[\frac{d\gamma_s}{d\tau} + \gamma_s \frac{d \ln[g_s z^2 K_2(z)/g]}{d\tau} \right]$$

We have considerable information on s/S .

Time evolution of s/S

$$\frac{d}{d\tau} \frac{s}{S} = \frac{g_s}{g} z^2 K_2(z) \left[\frac{d\gamma_s}{d\tau} + \gamma_s \frac{d \ln[g_s z^2 K_2(z)/g]}{d\tau} \right] \quad z = \frac{m_s}{T}$$

$$\frac{d\gamma_s}{d\tau} + \gamma_s \frac{d \ln[g_s z^2 K_2(z)/g]}{d\tau} = \frac{A_G}{2n_s^\infty} [\gamma_G^2 - \gamma_s^2] + \frac{A_q}{2n_s^\infty} [\gamma_q^2 - \gamma_s^2]$$

To integrate the equation for s/S we need to understand $T(\tau)$.

We have at our disposal the final conditions: $S(\tau_f)$, $T(\tau_f)$ and since particle yields $dN_i/dy = n_i dV/dy$ the volume per rapidity, $\Delta V/\Delta y|_{\tau_f}$. Theory (lattice) further provides Equations of State $\sigma(T) = S/V$. Hydrodynamic expansion with Bjørken scaling implies strictly $dS/dy = \sigma(T) dV/dy = \text{Const.}$ as function of time.

$dV/dy(\tau)$ expansion completes the model.

$$\frac{dV}{dy} \propto A_\perp(\tau) dz/dy|_{\tau,y}$$

a) we need transverse area expansion, $A_\perp(\tau)$. We assume $R_\perp(\tau) = R_0 + v_\perp(\tau)\tau$ and consider two geometries:

i) $A_\perp = \pi R_\perp^2(\tau)$ bulk expansion

ii) $A_\perp = \pi [R_\perp^2(\tau) - (R_\perp^2(\tau) - d)^2] = 2\pi d [R_\perp(\tau) - \frac{d}{2}]$ and

b) we need to associate with the domain of observed rapidity Δy a geometric region at the source Δz . We take scaling Bjørken hydrodynamical solution:

$$\frac{dz}{dy} = \tau \cosh y.$$

Early time behavior $\gamma_G(\tau)$ and $v(\tau)$ can be shown to be of minimal relevance. Strangeness looks back at times $\tau \simeq 2 - 3$ fm. Beyond, for yet earlier τ there is little, if any, memory.

Model of temporal evolution of Temperature

To integrate the equation for s/S we need to understand $T(\tau)$.

We have at our disposal the final conditions: $S(\tau_f)$, $T(\tau_f)$ and since particle yields $dN_i/dy = n_i dV/dy$ also the volume per rapidity, $\Delta V/\Delta y|_{\tau_f}$. Theory (lattice) further provides Equations of State $\sigma(T) = S/V$. Hydrodynamic expansion with Bjørken scaling implies **STRICTLY** $dS/dy = \sigma(T)dV/dy = \text{Const.}$ as function of time.

$dV/dy(\tau)$ expansion completes the model. This allows to fix $T(\tau)$.

$$\frac{dV}{dy} = A_{\perp}(\tau) \left. \frac{dz}{dy} \right|_{\tau=\text{Const.}} . \quad \text{Bjørken : } z = \tau \sinh y \rightarrow \left. \frac{dz}{dy} \right|_{\tau=\text{Const.}, y=0} = \tau$$

We consider two transverse expansion pictures: bulk and donut (d scales with R_{\perp}):

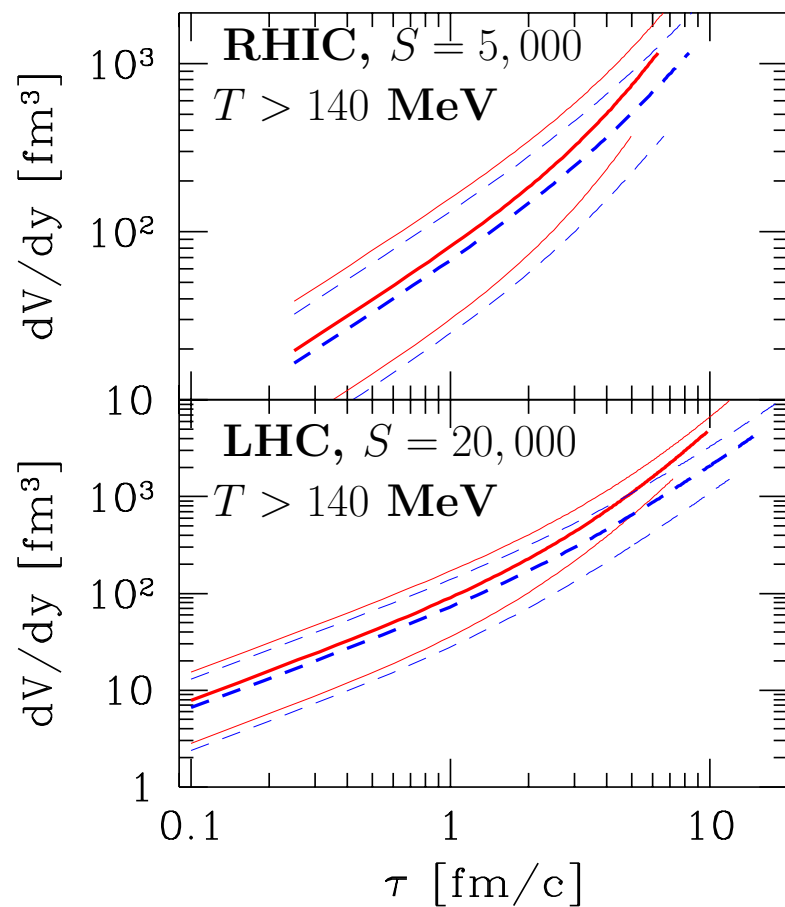
$$A_{\perp} = \pi R_{\perp}^2(\tau) \quad \text{or} \quad A_{\perp} = \pi [R_{\perp}^2(\tau) - (R_{\perp}^2(\tau) - d)^2]$$

We do assume gradual onset of expansion - hydro motivated:

$$v(\tau) = v_{\max} \frac{2}{\pi} \arctan[4(\tau - \tau_0)/\tau_v]$$

Values of v_{\max} we consider are in the range of 0.5–0.8 c , the relaxation time $\tau_c \simeq 0.5$ fm, and the onset of transverse expansion τ_0 was tried in range 0.1–1 fm.

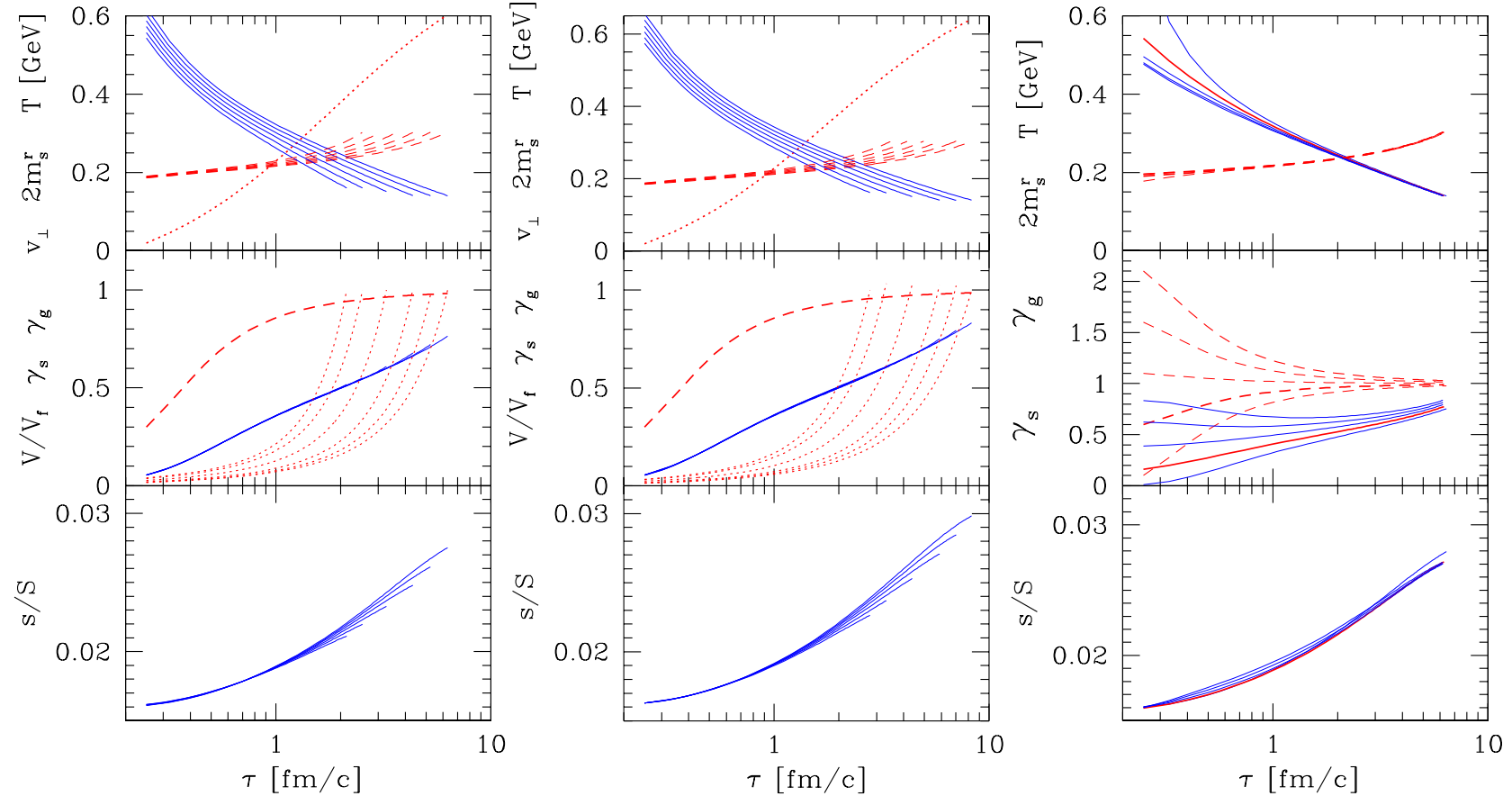
We took $R_{\perp}(\tau_0) = 5$ fm for 5% most central collisions. For centrality dependence, We further scale the initial entropy as function of centrality to assure $\frac{dS}{dy} \simeq 8(A^{1.1} - 1)$ which we found in the centrality data analysis.



Three centralities: middle $R_{\perp} = 5$ fm and the upper/lower lines corresponding to $R_{\perp} = 7$, and, $R_{\perp} = 3$ fm/c. dashed lines for donut geometry $d = 2.1, 3.5$ and 4.9 fm.

Main difference LHC to RHIC, lifespan much longer, despite increase of average final expansion velocity from 0.6 to 0.8 c.

s/S and γ_s at RHIC: centrality dependence



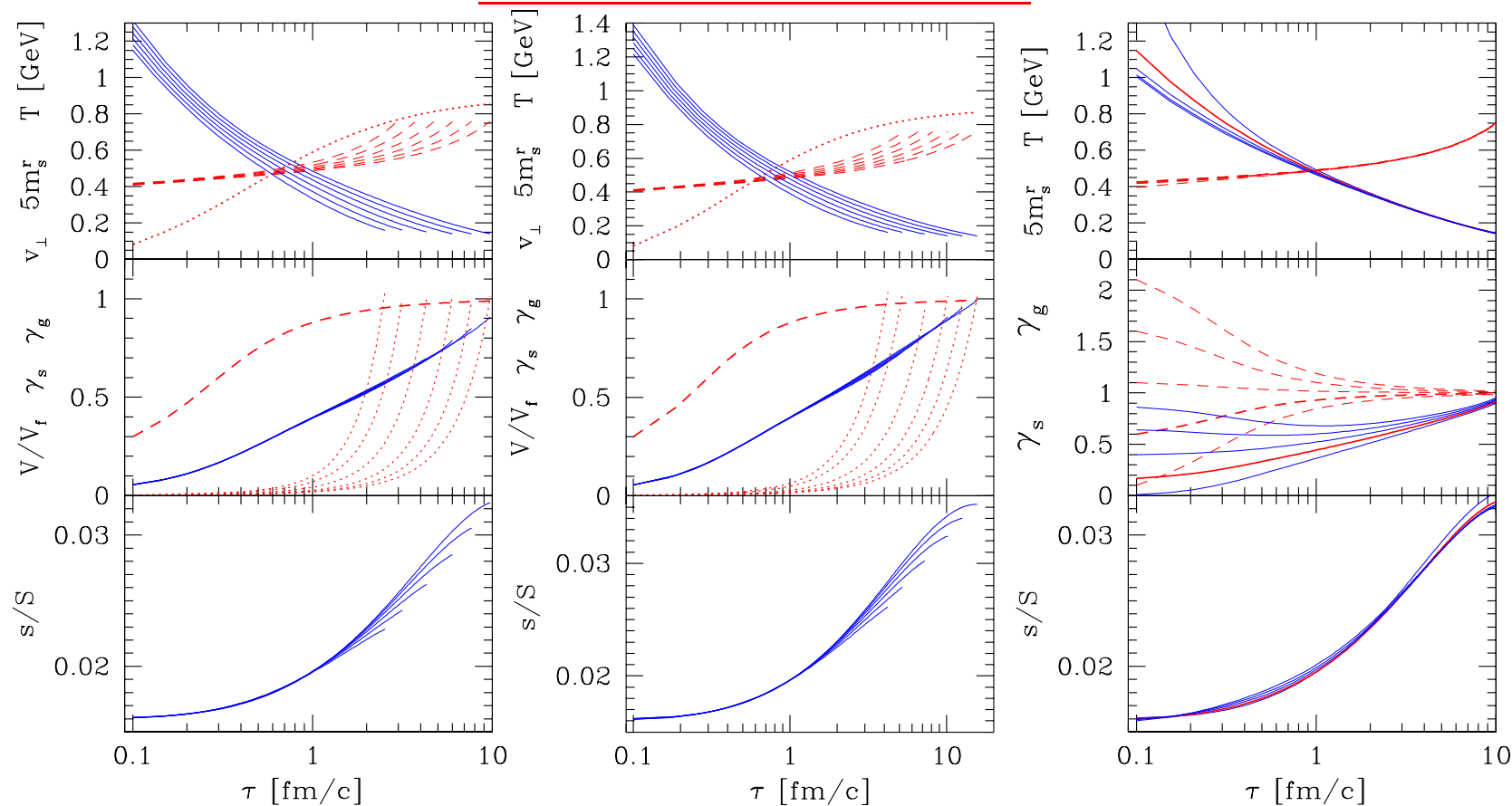
The two left panels: Comparison of the two transverse expansion models, bulk expansion (left), and wedge expansion. Different lines correspond to different centralities. **On right:** study of the influence of the initial density of partons.

Top: T , **middle** γ_s and **bottom** s/S

Assumptions:

dotted top panel: profile of $v_{\perp}(\tau)$, the transverse expansion velocity; middle panel: dashed $\gamma_g(\tau)$, (which determines slower equilibrating γ_q dotted: normalized $dV/dy(\tau)$ normalized by the freeze-out value.

What this means for LHC



Comments (same LHC and RHIC):

Top Panel: Initial temperatures accommodate $dS/dy|_f$ beyond participant scaling.

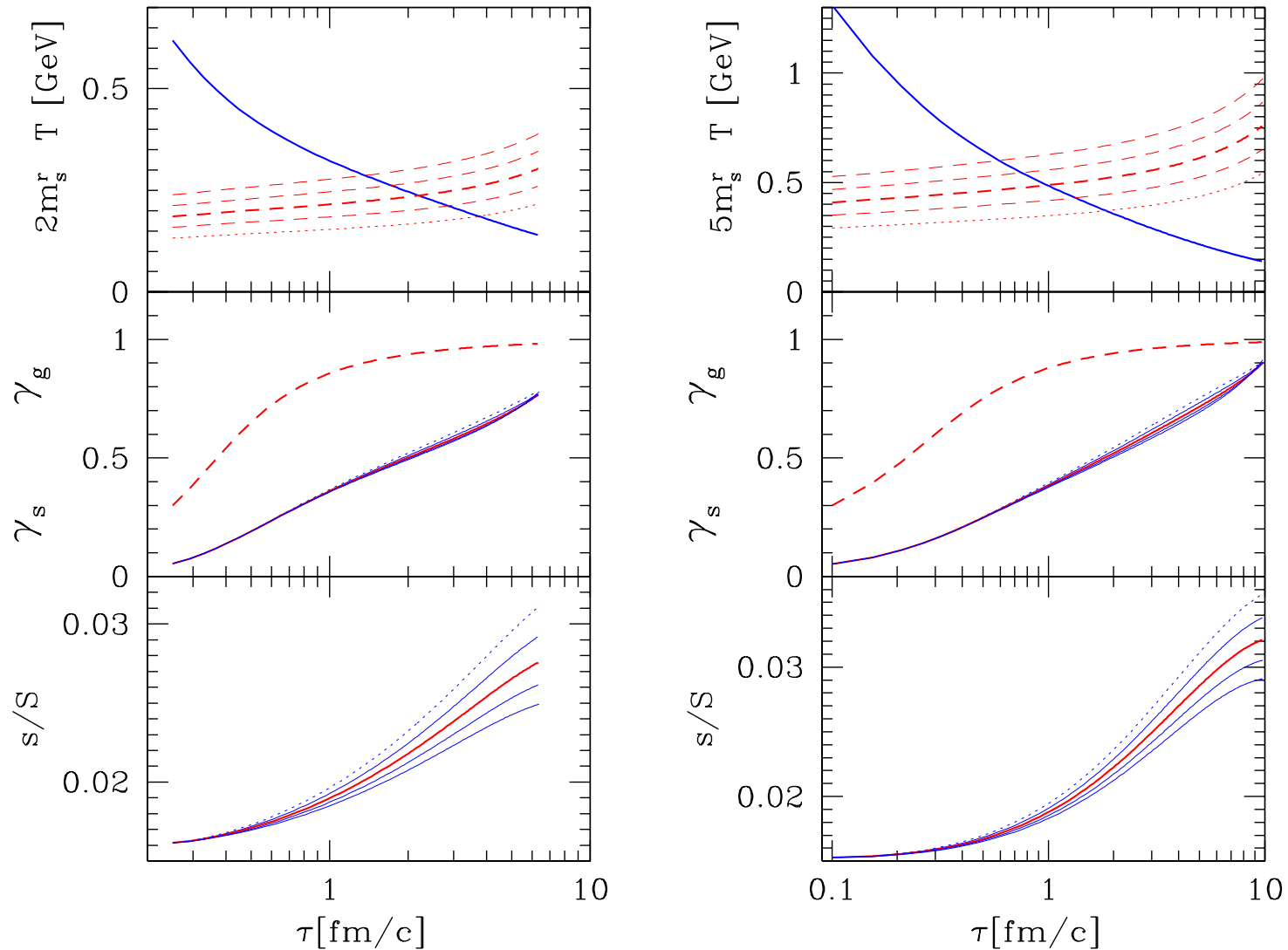
Middle Panel: Solid line(s): resulting γ_s for different centralities overlay;

Bottom panel: resulting s/S for different centralities, with R_0 stepped down for each line by factor 1.4.

Notable LHC differences to RHIC: (we assumed $dS/dy|_{\text{LHC}} = 4dS/dy|_{\text{RHIC}}$)

- There is a significantly longer expansion time to the freeze-out condition (factor 2).
- There is a 20% growth in s/S
- There is a significant increase in initial temperature to accommodate increased entropy density.

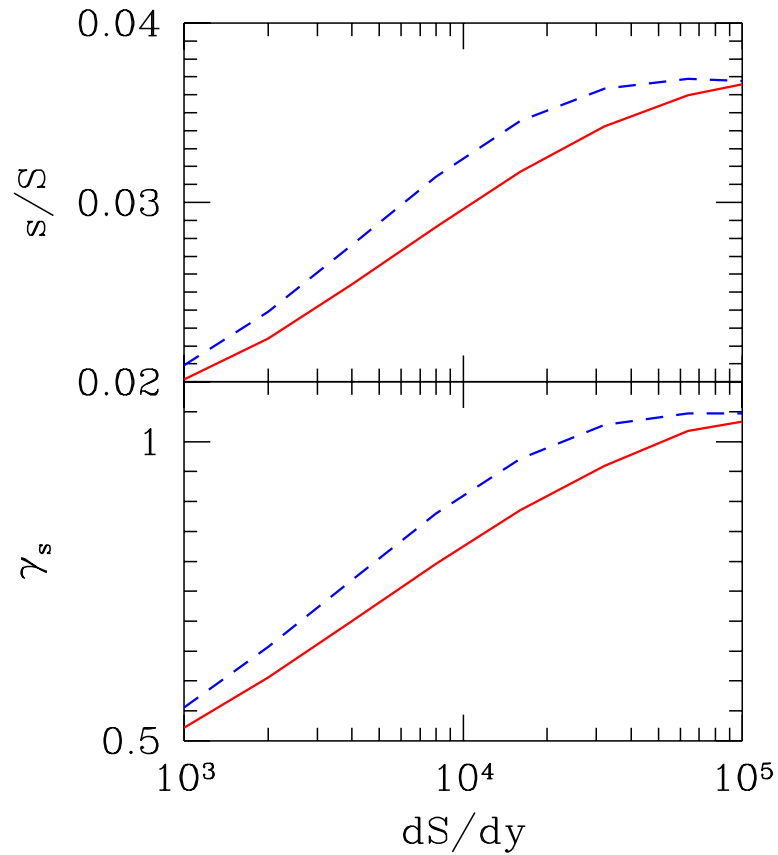
Strange quark mass matters



Left RHIC, right LHC, bulk volume expansion. m_s varies by factor 2.

γ_s overlays: **Accidentally two effects cancel: for smaller mass more strangeness production, but by definition γ_s smaller. s/S of course bigger for smaller**

A first look at energy dependence



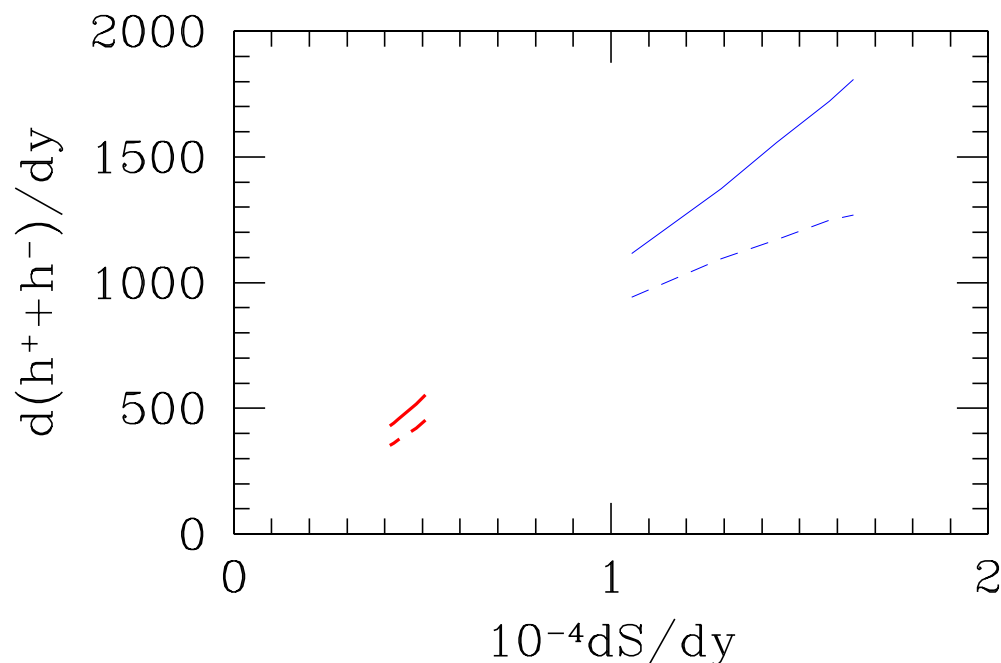
Solid, bulk expansion, dashed donut expansion.

Since the main parameter controlling the reaction energy dependence is the value of entropy (hadron multiplicity) produced, and we already have two points $dS/dy=5,000$ and $20,000$ (LHC) we complete for central collisions the results.

QGP equilibrates gradually, some over-equilibration for large entropy content.

Soft (strange) hadrons at LHC– predictions

For orientation: relationship of multiplicity to dS/dy



The

yield of charged hadrons $d(h^- + h^+)/dy$ for different values of dS/dy . Solid lines: after all weak decays, dashed lines: before weak decays. Left domain for RHIC and right domain for LHC - defined at $E/b = 40, 412$ GeV respectively, obtained not as fit to data but assuming $E/TS = 0.78$, baryon conservation etc. See: hep-ph/0506140 and Eur. Phys. J. C (2005) -02414-7 by JR and JL “Soft hadron ratios at LHC”

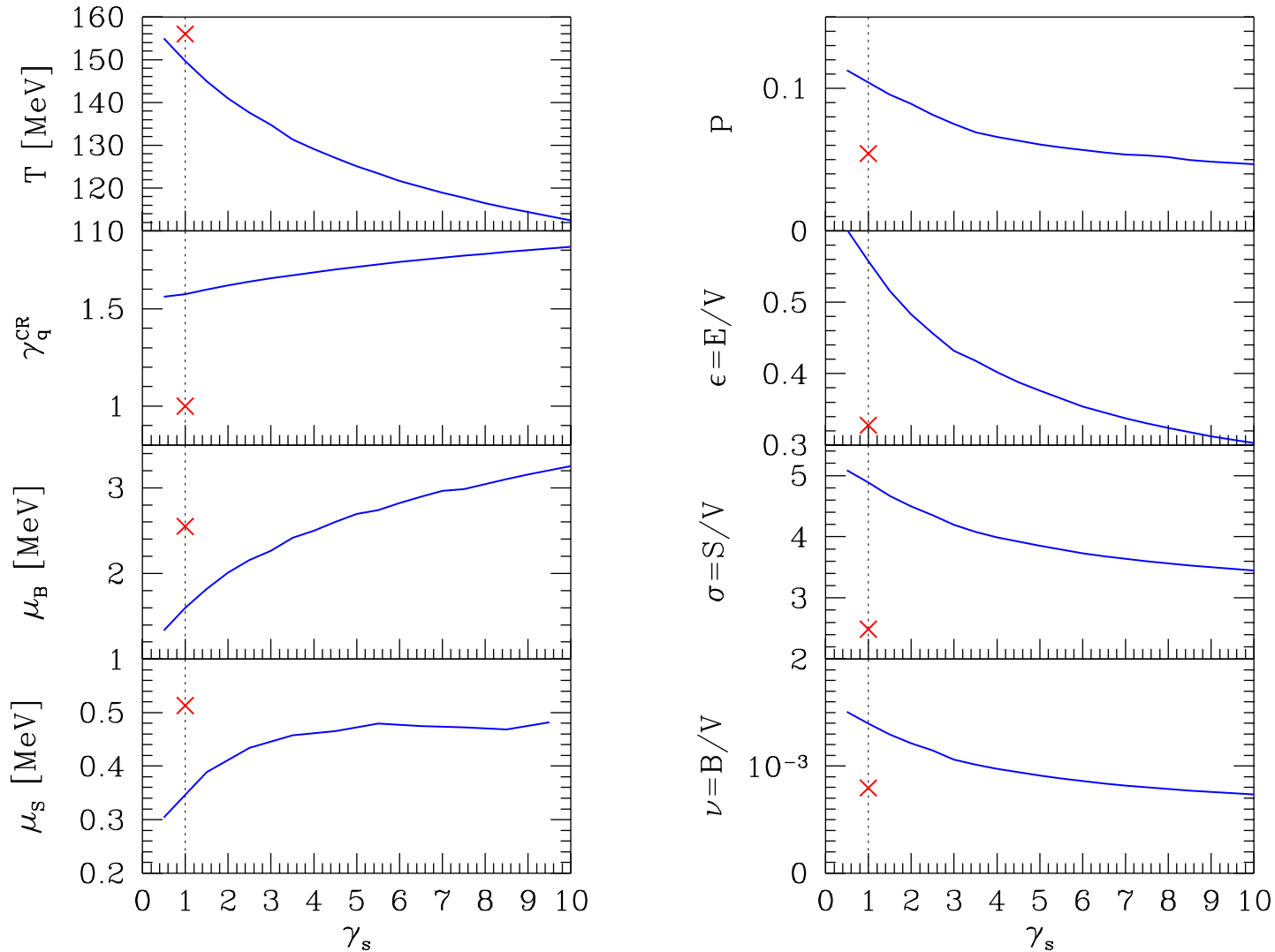
Assuming that statistical hadronization model applies, we have 7 parameters needing fixing:

- 1) $\mu_b \equiv T \ln(\lambda_u \lambda_d)^{3/2}$, the baryon and
- 2) $\mu_S \equiv T \ln[\lambda_q/\lambda_s]$, hyperon chemical potentials;
- 3) $\lambda_{I3} \equiv \lambda_u/\lambda_d$, a fugacity distinguishing the up from the down quark flavor;
- 4) γ_s the strangeness phase space occupancy;
- 5) γ_q the light quark phase space occupancy;
- 6) T , the (chemical) freeze-out temperature;
- 7) dV/dy , the volume related a given rapidity to the particle yields;

There are several constraints and physical conditions:

- 1) What is baryon stopping? use $dE/db = 412 \pm 20$ GeV, μ_b is hard to measure .
- 2) Strangeness conservation, we set $(\bar{s} - s)/(\bar{s} + s) = 0 \pm 0.01$, this fixes μ_S given μ_b .
- 3) The electrical charge to net baryon ratio, we set $Q/b = 0.39 \pm 0.01$. Fixes λ_{I3}
- 4-5) The value of γ_s^h will be varied, the value of γ_q^h set either to unity (for equilibrium) or max allowed value 1.6–1.7.
- 6) We rely on $E/TS \rightarrow 0.78$ for non-equilibrium and $\rightarrow 0.845$ for equilibrium
- 7) particle ratios limit need for volume normalization.

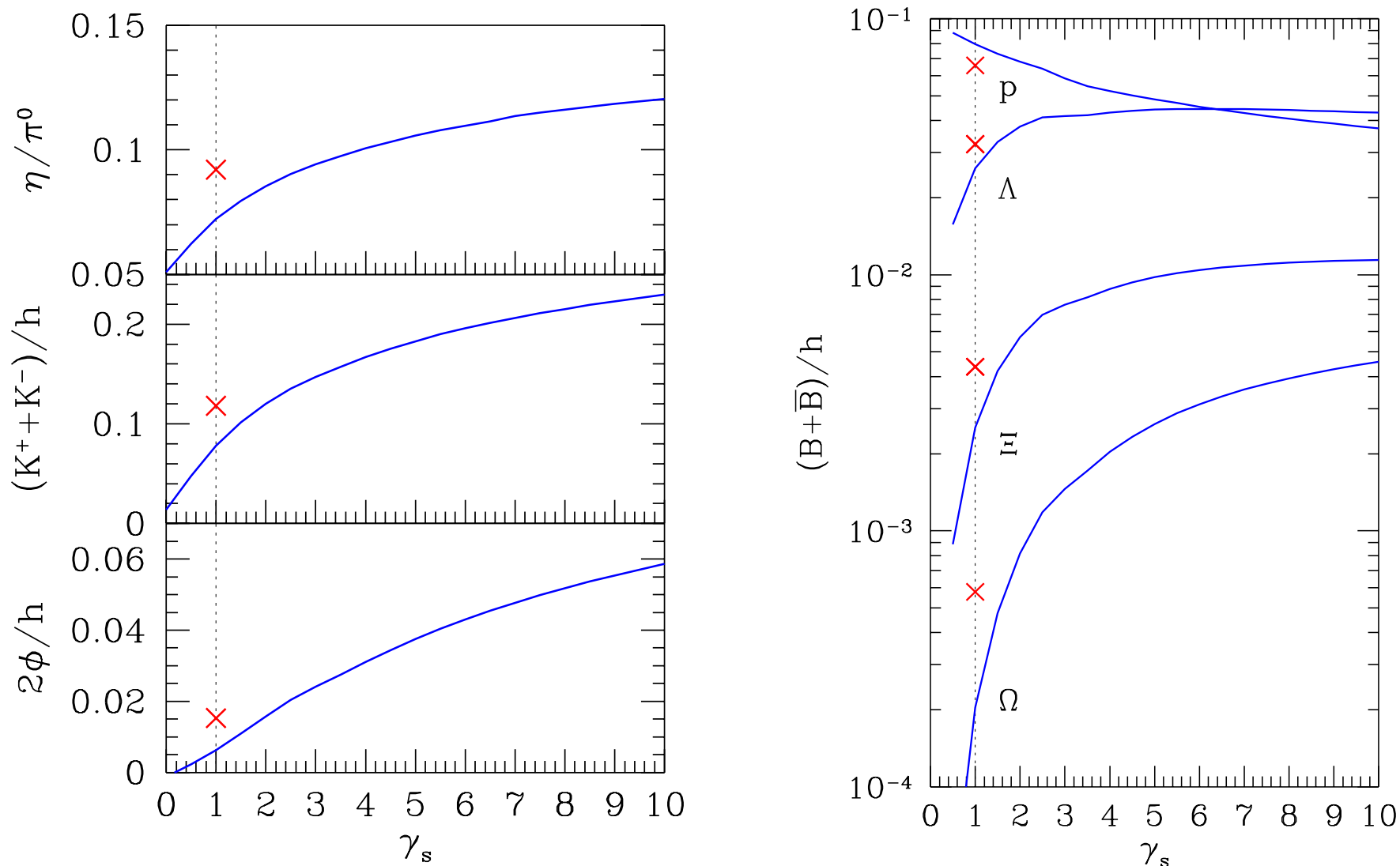
Range of Parameters / Physical Freeze-out Conditions at LHC



On left: The values of T , γ_q^{CR} , μ_B , and μ_S as function of varying γ_s , the equilibrium model results are crosses at $\gamma_s = 1$ for $\gamma_q = 1$.

On right : Pressure P [GeV/fm³], energy density ϵ [GeV/fm³], entropy density $\sigma = S/V$ [1/fm³], net baryon density $\nu = (B - \bar{B})/V = b/V$ [1/fm³], for non-equilibrium SHM. Cross at γ_s for chemical equilibrium.

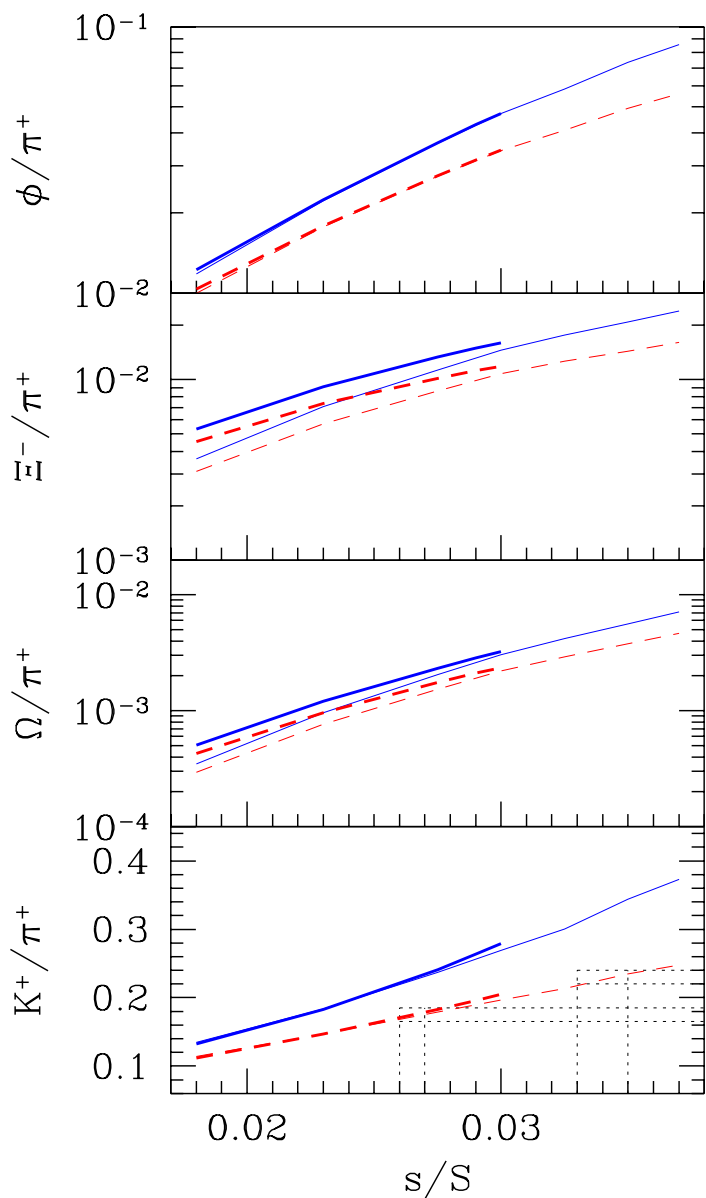
Particle ratios at LHC



All yields after weak decay of hyperons and $K_{S,L}$, crosses denote chemical equilibrium result. $h = h^+ + h^- \equiv p + \bar{p} + \pi^+ + \pi^- + K^+ + K^-$, NEXT PAGE: all yields BEFORE weak decays.

$dV/dy =$ $=3600 \text{ fm}^3$ dN/dy s/S	$T = 156$ $\gamma_s^H = \gamma_q^H = 1$ $\mu_B = 2.57, \mu_S = 0.51$	$T = 145$ $\gamma_s^H = \gamma_q^H = 1.62$ $\mu_B = 1.83, \mu_S = 0.40$	$T = 135$ $\gamma_s^H = 3, \gamma_q^H = 1.67$ $\mu_B = 2.28, \mu_S = 0.45$	$T = 125$ $\gamma_s^H = 5, \gamma_q^H = 1.73$ $\mu_B = 2.70, \mu_S = 0.48$
	0.025	0.021	0.029	0.034
π^+	466.22	866.24	655.12	506.6
π^-	480.48	889.48	682.24	535.6
π^0	524.98	966.74	751.16	598.4
K^+	84.60	137.62	163.48	176.9
K^-	84.16	136.98	162.54	175.8
K_S	81.96	133.42	156.82	168.1
ϕ	10.95	15.73	26.86	36.54
p	32.80	64.98	36.12	19.98
\bar{p}	31.76	63.42	34.96	19.18
$\bar{\Lambda}$	16.76	32.24	28.34	21.9
$\bar{\Lambda}$	16.33	31.62	27.58	21.1
Ξ^-	3.12	5.94	8.46	9.46
Ξ^+	3.06	5.86	8.28	9.20
$\bar{\Omega}$	0.416	0.724	1.634	2.56
Ω	0.410	0.718	1.610	2.52
$K^0(892)$	24.78	35.58	35.34	31.2
$\Delta^0 = \Delta^{++}$	6.16	11.66	5.68	2.70
$\Lambda(1520)$	1.29	2.220	1.66	1.08
$\Sigma^-(1385)$	2.14	3.98	3.28	2.34
$\Xi^0(1530)$	0.914	1.656	2.26	2.46
η	59.6	95.2	93.4	90.2
η'	5.32	7.62	7.78	7.06
ρ^0	53.8	79.2	48.4	29.8
$\omega(782)$	49.8	72.2	42.4	25.0
$f_0(980)$	4.50	6.42	6.28	5.44

Multi strange hadrons are more sensitive to s/S

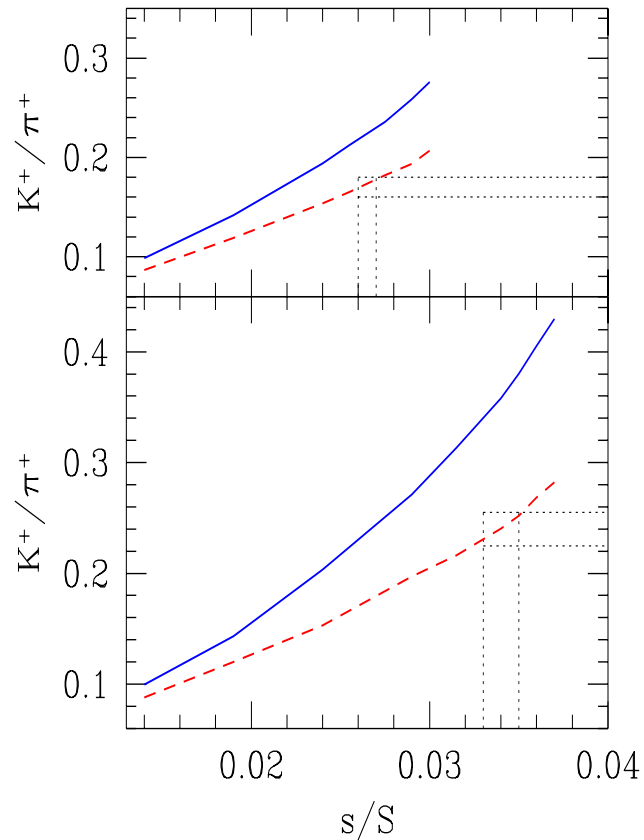


Top three panels:
 Φ/π^+ , Ξ^-/π^+ , Ω^-/π^+ (log scale)
 relative yields of multi strange
 hadrons, as function of s/S
 Φ/π^+ , Ξ^-/π^+ , Ω^-/π^+ (log scale).

Solid lines primary relative
 yields, dashed lines after all weak
 decays. Thick line with $s/S < 0.3$
 are for RHIC and thin lines are
 for LHC physics environment.

Bottom panel: restating for
 comparison K^+/π^+ .

How much enhancement in K/π ?



K^+/π^+ ratio as function of attained specific strangeness at freeze-out, s/S . Solid lines bare yields, dashed lines after all weak decays have diluted the pion yields. Top for RHIC and bottom for LHC physics environment. An increase by about 40% is predicted from $K^+/\pi^+ = 0.17$ at RHIC to $K^+/\pi^+ = 0.24$ at LHC. If LHC is subject to donut-expansion, increase more significant.

Hadronic/ flavor QGP signatures future challenges:

- RHIC * charm production, thermalization, **recombination** ;
- * background from hadron decays into dileptons and photons: search for kinematic niches where **glowing plasma** is visible.
- LHC * Violent expansion of over-saturated QGP: resonances, statistical hadronization, bulk matter dynamics, critical (phase boundary) **chemical nonequilibrium** ;
- * Mixed charm-bottom states $B_c(b\bar{c})$ will be made relatively abundantly (comparing to pp) in the quark soup at LHC, this opens up **laboratory of atomic QCD** ;
- * Charm and bottom yield at LHC: also in depth tests of **small- x** structure functions
- SPS * search for **onset of deconfinement** as function of energy and of system size.

Conclusions

- Strangeness experimental results fulfill all our expectations: resounding confirmation of fast hadronization of quark-gluon plasma.
- Full analysis of strangeness and hadron energy excitation functions and centrality dependence is now available.
- Strangeness equilibration can impact phase boundary and transition properties: QCD matter with 2+1 flavors exceptionally fine tuned.
- Evidence for CHEMICAL equilibration of the QGP at RHIC; but not in final state hadrons which abundances are controlled by prevailing valance quark yields.
- QCD based kinetic evaluation of the two QGP global observables γ_s and s/S produces strangeness enhancement – additional strangeness beyond initial state. Enhancement by a factor 1.6-2.2 for s/S seen.
- QCD kinetic model tuned to describe strangeness at RHIC, predicts further increase of specific enhancement at LHC with strong additional enhancement of multi strange hadrons and some noticeable increase such as in K^+/π^+ .